Hydrophobic Effects and Modeling of Biophysical Aqueous Solution Interfaces

Lawrence R. Pratt*,† and Andrew Pohorille*,‡

Theoretical Division, Los Alamos National Laboratory, Los Alamos, New Mexico 87545, and NASA, Ames Research Center, Exobiology Branch, Moffett Field, California 94035

Received March 7, 2002

Contents

* To whom correspondence should be addressed.
† Los Alamos National Laboratory.
‡ NASA, Ames Research Center.

1. Introduction

As hydration contributions to stability of macromolecular assemblies in aqueous solution, hydrophobic effects are virtually universally acknowledged. Hydrophobic effects are widely believed to stabilize folded structures of globular proteins.[1,2] More straightforwardly, hydrophobic contributions drive the formation of micelles and bilayer membranes.[3] These topics are frequently central to discussions of the origin of life.[4−6]

It has long been obvious that hydrophobic effects can exhibit an impressive variety of expression and context. In molecular terms, the conceptual chain from the solubility of inert gases to the formation of micelles and membranes to the structures of soluble proteins is extended and branched. Small hydrophobic solutes in water and extended interfaces of water with organic solutions, membranes, or biological macromolecules form opposite ends of a spectrum of possibilities. The connections between these limiting cases have not been reviewed recently, and the role of hydrophobic effects in mediating phenomena at aqueous interfaces has received relatively little attention compared to other aspects of hydrophobic behavior.

The past decade has seen compelling progress in the molecular theory of the most primitive of hydrophobic effects, those of submacromolecular scale.[7,8] At the same time, substantial theory and modeling results have accumulated on hydrophobic effects associated with solution surfaces and macromolecules. This article reviews the latter results from the perspective of the recent progress with small molecule problems. Our goal is to assist consolidation of small-molecule-scale theories of hydrophobic effects with concepts of hydrophobic effects at a supermolecular scale.

1.1. Definition of Subject Reviewed

Specifically, we review theory and modeling results on surfaces of liquid water contacting materials of biophysical interest. Our plan is to start with the simplest instances of water in contact with hydro-

10.1021/cr000692+ CCC: $39.75
Published on Web 07/16/2002

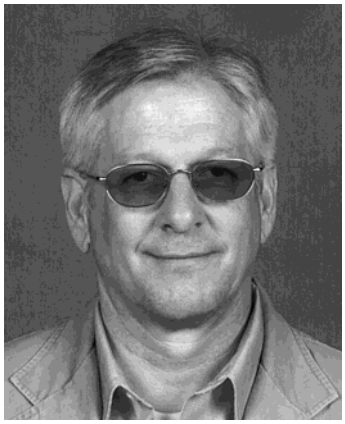

Lawrence Pratt is a Technical Staff Member in the Theoretical Chemistry and Molecular Physics Group (T-12) at Los Alamos National Laboratory. He received his B.S. degree in Chemistry from Michigan State University in 1972 and M.S. (1974) and Ph.D. (1977) degrees in Physical Chemistry from the University of Illinois. After holding positions at Harvard and U.C. Berkeley, he has been at Los Alamos since 1984. His research focuses on theoretical problems in chemical physics but especially theory of molecular solutions and hydration problems in molecular biophysics.

Andrew Pohorille received his Ph.D. degree in Biophysics from the Department of Physics, University of Warsaw, in 1979. He obtained his postdoctoral training with Professor Bernard Pullman at the Institute de Biologie Chimico-Physique in Paris. Between 1982 and 1992 he was on the research faculty at the Department of Chemistry, University of California at Berkeley. Since 1992 he has been Professor of Chemistry and Pharmaceutical Chemistry at the University of California at San Francisco. He joined the staff of the Exobiology Branch at NASA-Ames in 1996. Currently he heads the NASA Center for Computational Astrobiology and Fundamental Biology. His main interests have been centered on simulating the structure and function of biomolecular and cellular systems, in particular membranes and membrane proteins. He also has a long-standing interest in the nature of hydrophobic effects and aqueous solution interfaces. His other research activities are devoted to computational modeling of genetic and regulatory networks, the mechanism of anesthetic action, the origin of life, and the structure of comets. He also works on the development of new computational methods and algorithms particularly suitable for parallel and distributed computing. He has co-authored over 70 peer-reviewed publications in these and related areas.

phobic materials and to proceed toward more complicated cases. Thus, we begin with water at idealized rigid inert walls. We consider the water liquid−vapor interfaces as the next simplest hydrophobic surfaces. Subsequently, we review molecular modeling of the progressively more complex systems including interfaces between liquid water and organic solvents, the disposition and interaction of molecular solutes at these interfaces, and concluding with polypeptides located at interfaces between water and lipid bilayers but focusing on the role of hydrophobic phenomena in considering these complicated systems.

Experimental results are included to the extent that they are directed toward the goal of molecular explanation. We exclude observational biophysical work, either by experiment or simulation, that does not principally address the foundational issue of understanding hydrophobic effects, even though molecular-scale biophysics may have been a dominating motivation for studies of hydrophobic phenomena. We also exclude the vast topic of interactions between surfaces separated by aqueous solutions, such as the interesting work with surface force[9] and osmotic stress techniques.[10] There are important areas of overlap between that work and the topics reviewed here, but that inclusion would make the present discussion impossibly large.

The remainder of this Introduction gives some orientation and preliminary materials that serves to express a current basis for understanding small molecule hydrophobic effects.

1.2. Orientation and Preliminaries

It has long been recognized that classic hydrophobic effects are sensitive to temperature.[11−15] Operationally, hydrophobic effects are broadly identified by the temperature signatures of large, negative entropies of solution and large, positive heat capacity changes upon dissolution.[14−17] One motivation for this review is that characteristic hydrophobic temperature dependences for small-molecule hydration have been substantially clarified in recent years. Whether and how these effects are present at aqueous interfaces is, however, not so clear. This may be a research issue in forthcoming years, and therefore, a summary of what is known on this subject may be helpful.

For definiteness, we can give some examples of the characteristic hydrophobic temperatures in supermolecular settings. Consider the process of micelle formation, conceptualized roughly as an inverse of hydrocarbon dissolution into water: "In all cases therefore the driving force for micelle formation is a positive entropy change, as is to be expected for a phenomenon that is a manifestation of the hydrophobic effect."[13]

This characteristic 'inverse' temperature effect can be demonstrated with proteins also, and a nice example is provided by elastin materials.[18] For example,[19] the simple polypeptide $(VPGVG)_{18}$, with no hydrophilic residues and indistinct secondary structure in solution, undergoes hydrophobic collapse when the temperature is increased from below to above the transition temperature of 27 °C. These particular temperature behaviors are often of qualitative importance: it now appears common for protein structures to unfold upon appropriate cooling.[20]

As we understand hydrophobic effects better, the complex interplay between interactions of different types presents itself in a more subtle light. Studies of the stabilities from proteins of hyperthermophilic organisms emphasize by contrast the broadest point that the full mixture of interactions is complicated: "...the identification of stabilizing interactions is a search for small differences against a huge background".[21] And it seems "nature has used all possible strategies to increase the T_m value of thermophilic proteins".[21]

1.2.1. Macroscopic Conceptualizations and Microscopic Progress

The most primitive concept of hydrophobic interactions is associated with oil−water fluid-phase separation. Without attempting a genuine history, we note here some historical contributions that serve to anchor current ideas. Franks[22] emphasizes that hydrophobic effects have been recognized and studied in the context of association colloids and micelles since the 1930s. Nevertheless, the broad view of hydrophobic effects now current was not always so

clear, particularly in regard to the structure and stability of soluble proteins. Kauzmann[23] coined the term "hydrophobic bond", and in the context of protein solution structure, that presentation has been a starting point for studies of hydrophobic effects. Tanford gives an interesting discussion of the context and views current to Kauzmann's treatment.[2]

In the absence of a full molecular understanding, hydrophobic effects have typically been viewed through macroscopic properties associated with liquid water which are regarded as unusual. Examples[24,25] are the dielectric constant[26−30] and the surface tension of liquid water with its vapor and with nonpolar fluids.[31,32] Structural, i.e., '*clathrate*', models and 'mixture' models were motivated by structural information on other aqueous phases. The 'shell models'[33−35] of hydration effects on biopolymers similarly attempted to avoid a direct molecular-scale confrontation with the complexities of the theory of liquid water. These approaches have not produced molecular insight into hydrophobic effects because, to the extent that they have been successful, they have avoided molecular theory. The recent progress hinted above[8,36] has been built from basic molecular theory but also has had empirical inputs including equation of state information, measured structural quantities, and the results of heuristic testing utilizing molecular simulation.

Some features of that basic molecular theory are likely to become broadly useful concepts and are used further in this review. Therefore, we give a simple introduction to these concepts.

1.2.2. Some Basic Results from Statistical Thermodynamics

A theoretical anchor for the results we wish to describe is the potential distribution theorem.[37,38] The quantity of primary interest is the partial molar Gibbs free energy or chemical potential of the solute in solution. For the generally interesting case of solutes with internal flexibility, this chemical potential can be completely, though somewhat formally, expressed as

$$\mu_i = kT \ln[\rho_i \Lambda_i^3/q_i^{\text{int}}] - kT \ln\langle\langle e^{-\Delta U/kT}\rangle\rangle_0 \qquad (1)$$

Here q_i^{int} is the partition function for a single solute molecule and the double brackets indicate averaging over the thermal motion of the solute and the solvent molecules under the condition of no solute−solvent interactions. ΔU is the potential energy of solute−solvent interactions. This quantity need not be pair-decomposable but is just the difference between the total interaction energy of the system and interaction energies of the separated solute and solution. The first term on the right side of eq 1 would be the result if there were no interactions between the solute and the solution. Thus, the second term describes those interactions and is the quantity of interest in considering hydration effects.

This result is called the potential distribution theorem because after writing

$$\langle\langle e^{-\Delta U/kT}\rangle\rangle_0 = \int P_0(\Delta U) e^{-\Delta U/kT} d(\Delta U), \qquad (2)$$

evaluations can be based upon the distribution function $P_0(\Delta U)$ of the interaction potential energy. This is analogous[38] to the textbook perspective on partition functions, e.g.

$$\int P_0(\Delta U) e^{-\Delta U/kT} d(\Delta U) \leftrightarrow \sum_i \Omega_i e^{-E_i/kT} \qquad (3)$$

These foundations have lead to progress because the necessary distributions can be modeled, compared to computer simulation results, and then revised and improved.

For idealized hydrophobic effects this heuristic process has gone as follows: The strictly hydrophobic case is one in which ΔU involves no classic electrostatic interactions, no hydrogen bonding, and no other chemical or associative interactions. ΔU is of van der Waals type. In the extreme model, ΔU involves only hard-core repulsions preventing overlap of van der Waals volume of any solution constituents with the van der Waals volume a solute molecule. In this case, the Boltzmann factor of eq 2 is zero for any sampled configuration that has such an overlap and is one otherwise.

Therefore, this formula collects the weight of all sampled configurations that have no van der Waals overlap; thus

$$\langle\langle e^{-\Delta U/kT}\rangle\rangle_0 = p_0 \qquad (4)$$

where p_n is the probability that n solution molecules overlap the solute in question and p_0 is the probability of zero overlaps. The distribution p_n then is modeled, and the initial efforts were based upon an information theory perspective[8,39] utilizing information from a variety of empirical sources.

This approach is consistent with the view that dissolving a solute can be considered as a two-step process. First, a cavity for the solute is created, and then the solute is placed in this cavity. The approach sketched here gathers statistical information from transient fluctuations and leads to a prediction of the likelihood of a fluctuation that would open a suitable cavity. Subsequent contributions from other interactions are typically interesting but are not addressed at this stage.

It is an important point for further theoretical progress that we have examples of the relevant distributions $P_0(\Delta U)$ corresponding to interactions of different types, e.g., classic electrostatic interactions and shorter ranged associative attractions.[38]

An important issue for the present review is that this approach carries through for spatially inhomogeneous systems also.[40−43] If the solute density is being tracked near an interface, e.g., by specification of a molecule-fixed center to produce an interfacial profile $\rho_i(z)$, then the partition function that is rightmost in eq 1 can be evaluated with that molecular center confined to a layer at z to produce a hydration free energy for solute molecules there. The Boltzmann factor of such hydration free energies then gives the density profile to within a normalization constant that is typically fixed by specification of the concentration in an adjoining bulk phase. This is based upon the principle that the chemical potential

on the left of eq 1 should be spatially constant. Therefore, if one of the factors on the right of eq 1 changes, the other factor has to change in a compensating way. This idea applies to conformational equilibrium also. If a solute has conformational coordinates $\mathscr{R}^n$ (this may include positioning of a molecular center also), then distribution in these coordinates can be obtained by calculations of free energies following along the lines of the potential distribution theorem.

1.2.3. Molecular Model of Hydrophobic Temperature Dependences

Returning to the hydrophobic temperature dependences, an explanation of those temperature dependences is now available[8,36,44] that is built upon molecular statistical thermodynamic basics presented above.

This explanation was a surprise, so an after-the-fact 'explanation of the explanation' sounds like 'rationalization'. However, it is worthwhile trying to give such a picture here.

A primitive observation is that the densities of most solvents decrease decisively with increasing temperature through physiologically relevant temperatures. The qualitative picture developed here is that relative to organic solvents, liquid water manages on the basis of a variety of tricks to limit the variation of the medium properties with changes of thermodynamic state, including temperature. Liquid water is unusual in having a limited region of density increase with increasing temperature and a higher critical temperature than the organic solvents to which it is typically compared. [The density increase is not solely the explanation we are developing but is just an example of a contrivance involved; the distance to the critical temperature is a dominating issue.] Again, relative to organic solvents, the compressibility of water is low in comparable terms; liquid water exhibits a minimum in its compressibility at 46 °C. The low compressibility limits variations of the medium properties with respect to isothermal density changes. [It is a remarkable fact that differences in experimental hydrophobicities between H_2O and D_2O can be nicely correlated with the differences in the experimental compressibilities of these liquids.[36]] This leads to a picture in which the aqueous medium is stiffer and expands with temperature less significantly than the natural comparative solvents. Then an increase in temperature can be mostly expressed as an increase in the kinetic pressure that the solvent exerts through collisions on these ideal, perfectly rigid hydrophobes. It is this that leads to the increased strength of hydrophobic effects with increasing temperature for temperatures not too high.

If a balancing act minimizing the variations of the medium properties with temperatures is possible, it should be a useful trick since it should have the consequence of expanding the temperature window over which biomolecular structures are stable and functional.

Note that hydrogen bonding, tetrahedrality of coordination, random networks, and related concepts are not direct features of this qualitative perspective.

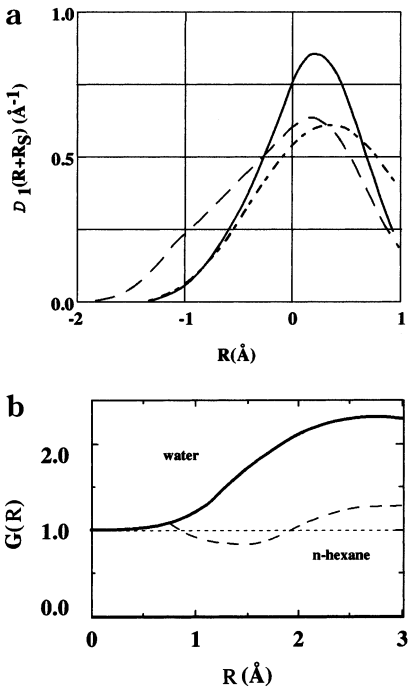

Figure 1. Example of statistical characterization of available space for inert spherical solutes in liquids, redrawn from refs 41 and 46. See section 1.2.2. (Top) The curves are water (—), *n*-hexane (- - -), and random−Hertz−distribution for the same density and R_S as water (- · -). (Bottom) The curves are water (—) and *n*-hexane (- - -).

Nevertheless, they are relevant to understanding liquid water; they are elements in the bag of tricks that is used to achieve the engineering consequences that are discussed in the picture above.

The stiffness concept involved in this explanation has been further characterized.[8,36,41,44−48] As an illustration, Figure 1 gives the quantity $\mathscr{D}_1(R) = -\partial p_0/\partial R$, with R the van der Waals diameter of an ideal, hard sphere hydrophobic solute. $\mathscr{D}_1(R)$ is the distribution of distances to the nearest atom center from an arbitrarily chosen point that is a candidate for insertion of a hard sphere solute. Offset by a van der Waals contact radius R_S these are distributions to the nearest van der Waals surface, a negative distance if the candidate point is inside the van der Waals volume. Observe that the most probable cavities are small as expected for a dense medium, in the neighborhood of 0.2 Å here. Notice also that the radius of the most probable cavities are about the same in water and *n*-hexane. Water is distinguished from the other alternatives here in the breadth of these distributions, i.e., liquid water is stiffer with respect to opening spherical cavities of substantial size.

Also shown in Figure 1 is the quantity $G(R) = -(4\pi R^2\rho_w)^{-1}\,\partial \ln p_0/\partial R$. Because this is the radius derivative of the hydration free energy for the hard core case, this quantity has been viewed as a 'compressive force' (in thermal energy units) exerted by the solvent on this hydrophobic solute. As is well-known, $G(R)$ is also the density of molecular centers, here the oxygen atoms, in contact with the sphere solute. Figure 1 shows that, for these atomic-sized spherical solutes, liquid water exerts a higher compressive force on the solute than does liquid *n*-

hexane. It is thus a sensible view that hydrophobic hydration 'squeezes-out' small inert solutes.[49]

Given this plateau in our understanding, many more details surface as interesting issues for further study. Examples are hydration of extended solution surfaces and drying,[50] the effects of dispersion interactions, applications to surfaces of complex composition[51] and to macromolecules of irregular shape,[52] the combining of hydrophobic and hydrophilic contributions in some seamless way, and context hydrophobicity.[53] The review that follows attempts to organize some of the available molecular information relevant to addressing these subsequent questions.

2. Aqueous Interfaces

Two broad types of models of interfaces between water and strictly nonpolar media have been studied. In the first type, the nonpolar phase is idealized as a solid wall, as might be appropriate for liquid water contacting a solid paraffin phase. In the second type, water coexists either with its vapor phase or with a fluid phase representing, for example, an organic liquid.

2.1. Water at 'Inert' Walls

The cases considered here are all idealized models to some extent. It is not uncommon to consider rigid walls that are perfectly impenetrable to water oxygen atoms. Then the pressure of the fluid is provided directly by the density of oxygen atoms in contact with the wall. However, walls that exert smooth repulsive forces on water molecules have also been treated as have cases including attractive wall−molecule interactions. In all these cases, the density profiles for atoms near the wall are the quantities of first interest.

References 54−63 encompassed an influential early phase of molecular simulation of water at extended hydrophobic surfaces. A number of important points, associated with concepts articulated earlier,[64] emerged from these calculations. Under conventional conditions of moderate temperature and low pressure, these calculations yielded a weak layering of water molecules in the direction perpendicular to the planar walls into the liquid. The work of Jonsson[54] utilized the MCY potential energy model for water molecule interactions; this model is known to have a higher pressure near the experimental triple point than does the ST2 model utilized by the other simulations. The calculation of ref 54 yielded a significantly higher water density near the wall than did other simulations. A simple inclusion of image charge effects[58] associated with a paraffin material augments the wall−water molecule interactions with additional attractive forces of substantial strength and long range. This also significantly enhanced the water density contacting the surface. These effects lead to consideration of the classic issues of van der Waals interactions that we do not pursue further.

Some calculations[54,57,61,62] treated interaction models in which forces between water molecules and the wall were exclusively repulsive. Attractive wall−molecule interactions of van der Waals type were included in other studies.[55,56,59,60] When electrostatic intermolecular water−water interactions describing hydrogen bonding were eliminated,[59] the radial layering markedly increased as did the conditional density of water molecules in contact with walls. Since, the electrostatic interactions serve to lower the pressure of the liquid, this is the expected behavior: introducing electrostatic (H-bonding) interactions lowered the pressure and induced a weak dewetting response.[59]

The discussion by Stillinger[64] had pointed out that if the conditions of the liquid water were adjusted to a liquid−vapor phase coexistence point and if the wall−molecule interactions corresponded to simple repulsive forces exclusively, then it would be reasonable to expect that the observed density profile would describe a vapor film next to the wall. The calculations discussed here are consistent with that expectation, though they were not focused directly on this point and thus the conditions required to observe this dewetting were not imposed with that goal in view.

Another important point resulted from the determination of the average number of hydrogen bonds that are formed by water molecules in proximity to such walls. Following the discussion of Stillinger,[64] a simple expectation is based upon the consideration of an imaginary cutting plane passing through a region of the isotropic liquid phase of water. If the physical wall had no more structural consequences than an idealized cleaving of liquid configurations at this cutting plane, then we would expect water molecules just next to the physical wall to make only one-half the number of H-bonds it would have in the bulk liquid. The observation is that interfacial water molecules in the outermost interfacial layers with appreciable population make about three-fourths of the bulk average number of H-bonds.[59] A definition of a formed H-bond is, of course, somewhat arbitrary, and for a particular definition the precise average will depend on other conditions of the calculation, e.g., the thermodynamic state. If liquid water is conceptualized as a tetracoordinate network, then a bulk water molecule that might typically make four H-bonds will give up one of those H-bonds in the interfacial region to form three. The significant result is that the observed fraction three-fourths is greater than the ideal one-half. Faced with the loss of H-bonds, interfacial water molecules compensate to avoid loosing as many as one-half of the H-bonds they might make in the isotropic liquid: "...for the planar hydrophobic surface, the sacrifice of one possible bonding interaction is required to maximize the total interaction"[59] as Figure 2 depicts. This requires some structural reorganizational in the interfacial region relative to bulk.

The picture in Figure 2 is consistent with probable orientations of molecular dipoles in the interfacial plane, but broadly distributed. This conclusion seems to be a general outcome of this work, though some problematic observations are noted below.

For inert gas solutes, crude conceptions of the hydration structure are different. In those cases, neighboring water molecules can arrange not to

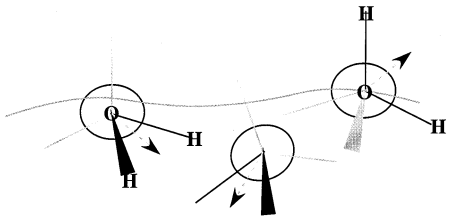

Figure 2. Idealized configuration for water liquid(below)−vapor(above) interface. These water molecules sacrifice one H-bond wholly. The arrows indicate dipole moments of these molecules; the picture suggests that molecular dipole moments may predominately form angles near 90° with the surface normal but with appreciable breadth in distribution. See sections 2.1 and 2.2.

sacrifice H-bonds. They can do that by orienting a tetrahedron face or edge (Figure 2) toward the center of the solute. Thus, the depiction of Figure 2 is of a "...resulting orientational structure that is inverted from that found for small solutes".[59]

Since the structures are different in these two cases, the questions naturally arise what intermediate circumstances are appropriate for the two cases and whether change from one case to another has any thermodynamic significance. These issues would be addressed by finding a method to change continuously from one case to the other. This can be done by considering an ideal spherical hydrophobic solute, call it A, of small size and examining the changes in hydration structure and thermodynamics as its size increases toward the planar surface (large radius) limit.[65−67] The revised scaled particle model[64] took no special account of such structural transitions; it describes a smooth, structurally unremarkable approach to the planar limit, and the detailed simulation checking of that form[67] has verified its quantitative accuracy. Therefore, a *direct* thermodynamic signature of such a structural change is not evident, although the temperature derivative of the hydration free energy (the hydration entropy) may well be different; that issue should be considered subsequently. Searches for structural observations of a transition are somewhat diffuse. In the small solute cases, the distribution of H atoms from the A center, $g_{AH}(r)$, shows some bimodality in the inner shell, i.e., $g_{AH}(r)$ has a broad and slightly split principal peak.[66,67] This is consistent with the structural picture of small solute hydration noted above. As the AO distance of closest approach increases, the AH principal peak broadens. This broadening eliminates the split and eventually, for hard spherical solute radii of nearly 10 Å, the inner shell peak becomes an nondescript mound. With this diagnostic, the transition is accomplished for A solute radii between 7 and 10 Å. Additionally, the density profiles obtained for spherical exclusion volumes are qualitatively different from that of a vapor−liquid interface when such spheres have radii between 6 and 7 Å.[65,67]

Conclusions are that these simplified pictures of hydration structure are qualitatively valid and may be helpful mnemonics. The literal situation, however, is statistically more complex than simple structural pictures suggest, and connections between the simple pictures and predictions of thermodynamic properties are subtle and nontrivial.

In this initial phase of simulation, the work of Valleau and Garder[62] brought some methodological questions to the foreground. In Monte Carlo simulation of liquid water between hard walls, they used a common potential energy model (TIPS2) but with minimum image treatment for intermolecular interactions of longer range than the cross-sectional scale of the simulation cell. Statistical convergence of the simulated properties was not obtained at 299 K, and results were limited then to more elevated temperatures. Even so, the expected equilibration of molecular orientations in a bulk liquid region was not observed. The issue of minimum image treatment of long-range interactions was the foremost concern discussed. Periodic boundary conditions do influence molecular orientational distributions even for short-range interactions, but those effects are typically not large.[68,69] It is worth noting that this intrinsic anisotropy is expected to vanish only as *all* dimensions of the simulation cell become macroscopically large. In addition, application of minimum image procedures to simulation of extended polar molecules raises some special issues related to the treatment of electrostatic interactions.[70] Indeed, subsequent work (below) has reaffirmed that the minimum image treatment of these interactions is the principal difficulty and in this setting produces a material akin to a liquid crystal between the plates.

A subsequent phase of simulation work on these problems substantially reinforced the picture described above.[71−80] Interaction models that include molecular polarizability have been studied[72] with the conclusion "...of quantitatively similar behavior for polarizable water compared to an effective pairwise additive model at a hydrophobic surface".

Integral equation theories have been applied to these problems also. The studies in refs 81−83 predict strong density oscillations in the vicinity of the wall, "...much stronger than one obtains from computer simulation techniques".[81] In contrast, Kinoshita and Hirata[84] predict weaker oscillations more consistent with the simulation results. The simulation of Spohr[77] was focused on checking the predictions of Booth et al.[83] That comparison suggested that the results for the density profiles were qualitatively different: highly structured in the integral equation approximation work but structured in the simulation only at the highest pressure treated. Shelley and Patey[75] describe their results as exhibiting "...strong long-lived fluctuations in the density profiles". However, the maximum oscillation amplitude in the density profiles is in the neighborhood of 20% of the bulk density, and this is a magnitude we classify here as 'weak' oscillations.

The role of the pressure of the liquid[85,86] and the attractive interactions between water molecules and the wall materials[86] has been the focus of some recent work. Bratko et al.[85] found that between two plates liquid water that is metastable with respect to evaporation can be sustained only if the interplate separation is greater than two molecular layers (for ambient pressures). However, at the higher pressure of 10^3 atm, two molecular layers of water could be sustained between the plates.

Zhu and Robinson[73] simulated water between rigid plates and utilized a minimum image treatment of electrostatic interactions as did Valleau and Gardner.[62] There were other differences between these two calculations, including the water model and the use of molecular dynamics rather than Monte Carlo approaches. Zhu and Robinson presented results for $T = 298$ K and did not comment on the difficulties encountered by Valleau and Gardner. In contrast, Shelley and Patey[75] explicitly studied the treatment of electrostatic interactions at the boundaries. They established that the minimum image treatment is the likely explanation of the difficulties identified by Valleau and Gardner and found the Ewald treatment of electrostatic interactions to be the preferred alternative.

It is difficult to compare the results of calculations by Galle and Vortler[87,88] with the work discussed above because their model is quite different from the more usual models that are the basis of the other work.

2.1.1. Model Hydrophobe and Water at Inert Walls

The studies of water at inert walls have been extended to treat the free energies of interaction of model atomic-sized hydrophobic solutes with these surfaces.[63,89,90] Wallqvist and Berne[63,89] used a sophisticated intermolecular potential energy model (RWK2-M) for water molecules but one for which less experience is available compared to most other models. In the absence of the model methane solute, the results obtained were reassuringly consistent with the body of previous work on this problem. Surprisingly, the model methane solute was found to be globally stable when positioned one water layer *into* the liquid phase, i.e., in a configuration solvent-separated from the wall. A later study[90] with a different potential energy model (ST2), which produced consistent results in the absence of the solute, found that most stable free energies were obtained when the atomic solute was in contact with the wall.

It is tempting to view these different outcomes in the context of the current speculations regarding pressure denaturation of proteins.[8,91] This is an issue for which historical views of hydrophobic effects had led to paradoxes.[92] A proposed resolution of those paradoxes is that pressure increases can change the relative stability of the contact and noncontact hydrophobic interactions, increasing the relative stability of the noncontact hydrophobic interactions. Then initial pressure denaturation, which has a different end point than thermal denaturation, can be sensitive to noncontact hydrophobic interactions. A physical view is that with increased pressure, water molecules can be jammed between hydrophobic contacts, leading to better stabilized solvent-separated hydrophobic interactions and to disrupted protein structures. Changes in the potential models might similarly lead to changes the relative stability of the contact and noncontact hydrophobic interactions. It is known that simulations of hydrophobic 'aggregation' with realistic but slightly different interaction models can show either dominating hydrophobic attractions or net repulsions.[8] The idea that noncontact hydrophobic interactions show more variability than the better described contact hydrophobic interactions is consistent with our present molecular understanding of hydrophobic effects.[8] This idea, however, has not been further checked in any specific sense.

The molecular-scale theory of hydrophobic effects has led to approximate approaches that can give a helpful perspective on the cases discussed above,[8] see section 1.2.2. It would be feasible to evaluate cavity-occupancy models for potentials of mean force for these cases, evaluate an inhomogeneous van der Waals contribution from solute−water dispersion interactions, and assess changes in hydration structure due to solute−water dispersion interactions.

2.2. Vapor–Liquid Water Interface

The next simplest interface of water with a 'hydrophobic' phase is liquid water with its vapor. In fact, this case is technically less complicated than the water−wall system. This is because no additional decisions are required to construct a model of the opposing phase and the vapor phase chosen is computationally simpler than any other choices. The initial study of this system was due to Wilson, Pohorille, and Pratt[93] but limited to 325 K for the TIP4P water model. The oxygen atom interfacial density profile was monotonic within statistical uncertainties with a central width $\approx$3 Å, slightly larger than a water molecular diameter. Water molecular orientational preferences were consistent with the results on inert walls, with the quantitative distinction that the distributions were more diffuse for the free interface. The strongest orientational preferences were observed for water molecules outside the central interfacial region. The outermost interfacial layers with nonnegligible population showed a weakly bimodal distribution of orientations of the OH bond, consistent with the idealization of Figure 2. Although water molecules showed only weak orientational ordering on the inner side of the central interfacial region, the density of molecular centers (here the oxygen atoms) was much higher and consequently the density of the perpendicular component of molecular dipole axes, referenced to those molecular centers, was highest through these inner-interface regions. The net orientation corresponded to a slight excess of molecular dipole axes vectors oriented inward, from the vapor toward the liquid phase.

A particular curiosity of this work was associated with the determination of the variation of the mean electrostatic potential through the interfacial region. This was *nonmonotonic*. Viewed physically, this result can be associated with the fact that for the models treated the two configurations suggested by Figure 2 are equivalent neither in energies nor in the extended charge distribution implied. A test charge approaching the liquid surface from the vapor first passes layers of excess positive charge with the compensating negative charges deeper into the interfacial region. This suggests that the rightmost configuration of Figure 2 is slightly more prevalent in the outermost interfacial layers with nonnegligible

population but, of course, the distributed partial charges for 'H-sites' and 'lone-pair' sites are not the same. In any case, the mean electrostatic potential first decreases into the liquid phase. On the other hand, for the more populated inner interfacial layers a slight net excess of molecular dipole axes are oriented inward, toward the liquid phase. Then a test charge passes positive charge layers last as it finally achieves the bulk liquid environment; the mean electrostatic potential finally increases toward the bulk liquid value. For this case, there is a mean electric field inversion in the interfacial region.

This description suggests a quadrupolar distribution of excess charge in the interfacial region. Indeed, it was later clearly articulated that this peculiar behavior was tied to the extended character of the molecule charge distribution that can be expressed by the molecular quadrupole moments.[94−96]

Note that the fundamentals for calculations of variation in a mean electrostatic potential through an interface are clear.[83,95−98] However, consensus on the practical calculation of these contact potential differences is not perfect. Formulas are sometimes adopted on an intuitive basis that depend on the choice of a molecular center.[99−101] In these cases it is reasonable to require that this choice is made clear.

Beyond the technical issues, it is striking that the natural descriptions here seem to rely on two 'subinterfacial regions', inner and outer interfacial regions, to convey both the orientational ordering and the observed mean excess charge densities.

Recent work has gone much further in documenting the description derived from simulations of thermodynamic properties of such two-phase systems, including phase coexistence as well as interfacial tensions. The correspondence of the simulation results with those thermodynamic properties is probably the first and most precise check to establish whether the simulations are relevant to understanding the 'experimental' liquid water/vapor systems. That is reviewed separately in section 2.2.1.

It is probably not surprising that treatment of electrostatic interactions has been a recurring issue for subsequent simulations of this interface. Ashbaugh[102] considered various truncations and assessed the variations of the orientational structure with changes in molecule centers used in truncations of electrostatic interactions. For the centers considered alternative to the conventional oxygen atom site, the orientational structure was somewhat diminished relative to the results based upon the oxygen atom center. Ewald treatments for slab geometries have been considered,[103−116] and these approaches are becoming standard methods.

Sokhan and Tildesley,[117] using the SPC/E model (see section 2.2.1 below), further validated several points made above. The net molecular dipole orientation density was toward the liquid phase. However, molecular dipolar orientations were predominately *parallel* to the interface and there was an inversion of the dipole orientation density in the interfacial region: molecules on the vapor side of the interface showed an enhanced tendency to orient their dipole axes out of the liquid phase, but that tendency was reversed for molecules on the liquid side of the interface. This situation was also observed in a Monte Carlo simulation utilizing the ab initio MCY potential model. Inclusion of polarizability in the TIP4P model affected this orientational structure only secondarily in that case.[118] Sokhan and Tildesley[117] also found an inversion of the mean electric field in the interfacial region but with a much weaker opposing feature on the liquid side of the interface than was seen in earlier calculations.[93] The interfacial thickness of this interface was about ≈3 Å at the lowest temperatures considered by Sokhan and Tildesley.[117] Additionally, they observed extremely weak oscillations of the interfacial oxygen density profile. The simulations were sufficiently long to consider the oscillations significant. In contrast, the simulation of Zhu et al.[119] produced a net dipole orientation opposite to those cited above.

da Rocha et al.[120] studied the interface between liquid water and CO_2 based upon the SPC/E model of water and a Lennard−Jones plus partial charge model (EPM2) of interactions associated with CO_2 molecules. The surface tensions computed at several state points were of the right magnitudes, and their changes with thermodynamic state reproduced trends found experimentally. The point with the best correspondence to experimental values had a tension approximately 25% too high. Strong orientational preferences at these interfaces for H_2O or CO_2 molecules were not observed. The water−carbon dioxide phase coexistence had been previously studied,[121] with favorable results, utilizing the SPC and TIP4P potential models and the same EPM2 model for CO_2.

Reassuringly, an 'ab initio' molecular dynamics calculation[122] agreed coarsely with previous simulations with regard to preferred orientations of water molecules near the air−water interface: some bimodality of molecular dipole orientations was observed in the outer interfacial layers but the orientations with molecular dipole axes toward the liquid seemed to predominate over orientations with molecular dipole axes close to the interfacial plane. 'Ab initio' molecular dynamics calculations offer an important new source of information on interfaces but are currently severely limited to small system sizes studied for short times. The work discussed here on the liquid water−vapor interface treated only 32 water molecules for times less than 7 ps, including equilibration time. Thus, even an accurate guarantee of the temperature consistency with the average mechanical kinetic energy is nontrivial. Here an average temperature was not given for the interface calculation. Because of such limitations "...it is not possible to produce realistic data for the water density distribution..."[122]

2.2.1. Validation of Simulation Models for Water Liquid–Vapor Coexistence

The most important point in this regard is that the SPC/E model[123] is now established as providing a reliable thermodynamic description of the liquid−vapor coexistence[124,125] to a surprising degree; the

computed critical temperature is accurate to nearly 1%. An earlier study of the SPC model indicated that the results, accurate at lower temperature, degraded somewhat at high temperatures.[126,127] The SPC/E model also provides an accurate prediction of the dielectric constant of the coexisting liquid along the saturation line,[124] and the calculated surface tensions are correct to within the modest statistical uncertainties of the calculations.[125] In the range 450 K < T < 600 K, liquid densities are slightly too small.[124,125]

Extensive consideration[128] of potential energy models that incorporate polarization features identified a dilemma but left it unresolved. In comparison to the well-known 'effective' potentials SPC and TIP4P, polarization models can do a better job for describing the liquid−vapor phase equilibrium at higher than ambient temperatures. However, the polarization models considered there[128] did a poorer job in describing familiar low-temperature properties of liquid water. Results for liquid−vapor phase equilibria based upon other polarization models were presented by Svishchev and Hayward.[129] A study[130] of an alternative style (TIP4P−FQ) polarization model suggested a prediction of the liquid−vapor critical point that was not as good. A model fitted directly to ab initio electronic structure energies for two-, three-, and four-molecule geometries performed less well than others in predicting the gas−liquid saturation line.[131]

A central force model of Stillinger−Lemberg type has been used to compute the liquid−vapor coexistence line.[132,133] The latter of these results is about as good as the SPC/E model. The suggested[133] critical temperature was too low by about 3%, the critical density was too high by approximately 5%, and the predicted critical pressure was too high by slightly more than 50%. The earlier of these efforts addressed the issue of the quantum mechanical nature of the thermal motion[132] utilizing a Feynman−Hibbs potential to capture the nonclassical features. In the historical sweep of understanding liquid water, these are secondary issues but probably important for the current interest in describing both high and low-temperature properties correctly.

2.3. Nonpolar Liquid–Liquid Water Interfaces

Molecular modeling of liquid−liquid interfaces has been reviewed by Benjamin.[134,135] Here we identify work particularly on interfaces between water and organic liquids.

Linse[136] used the MCY model potential for water−water interactions with the consequence that the density of the coexisting liquid water was too low by about 25% at the studied temperature of 308 K. Even so, the structuring of water molecules near this benzene−water liquid−liquid interface were reasonably similar to those of Lee et al.[59] corresponding to a rigid wall−water surface. The interface was observed to be molecularly sharp.

Simulations of the water−dichloroethane interface[137] raised some new issues: the influence of water on the structure of an organic liquid in the interfacial region. It was shown that both the orientations and conformations of dichloroethane were affected by the presence of water. In particular, a shift in the gauche/trans equilibrium toward the more polar gauche rotamer was observed at the interface with the aqueous medium. This is consistent with the idea that an environment of polar liquids should preferentially stabilize polar conformations.

Carpenter and Hehre[138] studied the liquid−liquid interface between water and *n*-hexane at $T = 299$ K using OPLS and SPC model potentials. In this case, the interface was significantly wider, approximately 10 Å, than in previous studies of liquid water interfaces in this temperature regime. As the authors correctly pointed out, this might be associated with the fact that the solubility of hexane in water described by this potential model seemed significantly too high. Perhaps for the same reason, orientational ordering of water molecules in this interface was not significant. However, the expected variation of hydrogen-bonding possibilities was still observed: fewer H-bonds were formed by interfacial water molecules, but those molecules were more efficient in H-bonding to the fewer near-neighbor water partners available.

Subsequent simulations of water−hexane and water−dodecane systems[42] yielded qualitatively different results. The water density profiles were found to be smooth, and the orientation of water molecules at the interfaces resembled closely that at the liquid−vapor interface. The density profiles of the two liquids exhibited some overlap. This overlap, however, was only limited, indicating that the liquids are indeed immiscible. This is shown in Figure 3.

One could interpret the overlap between the density profiles as an indication of molecular-level interpenetration between the two liquids in contact. Alternatively, the overlap could simply arise from spatial and temporal averaging of thermal fluctuations superimposed on a molecularly sharp interface. This issue was already raised, and largely resolved, in the early simulations discussed above.[42,136,137] In particular, Benjamin[42] performed an analysis similar to the coarse-graining procedure used by Weeks[139] to derive a capillary wave model. The results were consistent with a picture of a locally sharp interface broadened by capillary waves but not with mixing of the two liquids in the interfacial region.

In a following paper, van Buuren et al.[140] studied water−decane interfaces at $T = 315$ K and explored parameter ranges for Lennard−Jones interaction contributions that might improve the fidelity of such simulations. They showed that modest changes in these parameters would bring the surface tensions and solubilities into agreement with experimental values. In those cases the interfaces were again molecularly sharp. They also noted that the mean dipole orientations of water molecules at these interfaces displayed the reversal that we have discussed above. Michael and Benjamin[141] reported similar observations with a similar force field model. The interfacial reversal was noted also by Zhang et al.[142] in a study of a water−octane interfacial system. That work found the surface tensions well described by the CHARMM force field used. The water−carbon tetrachloride system has been studied on the basis

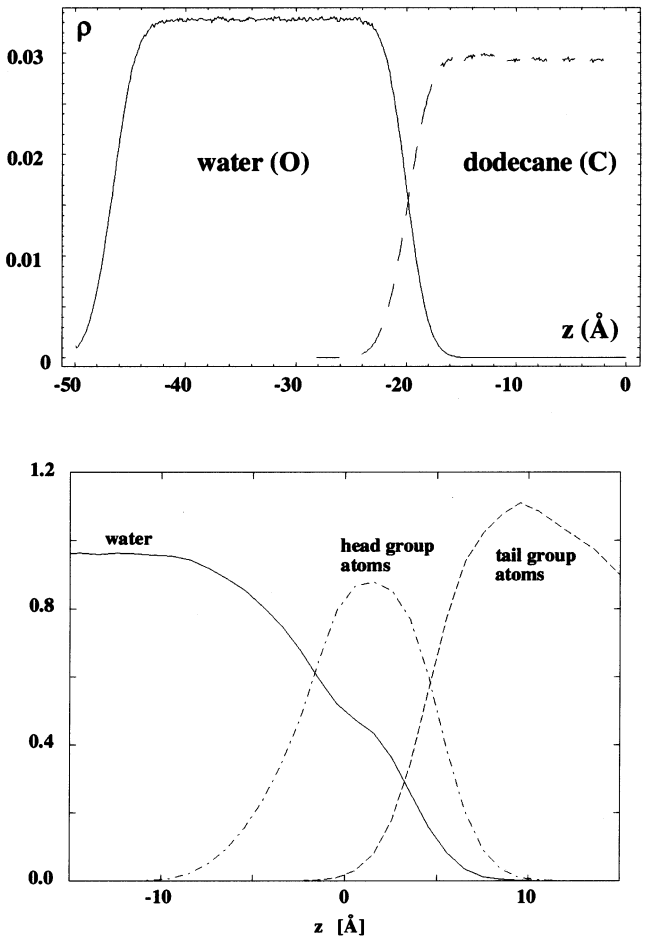

Figure 3. Density profiles of water oxygen atoms and methyl/methylene groups of dodecane at the water−dodecane interface (upper) or heavy atoms in headgroups and tails of POPC membrane (lower). $z = 0$ is at the equimolar surface of water for the lower panel. The profile for tail atoms of POPC extends to the center of the bilayer, approximately 18 Å from the interface. Note that water penetrates strongly the headgroup region of the membrane strongly but its hydrocarbon core only weakly.

of a force field that included molecular polarizability.[143] This interface too was viewed as molecularly sharp and interfacial water molecules H-bonded more efficiently to the reduced number of water molecule neighbors available. The recent work of Senapati and Berkowitz[144] on the liquid water−carbon tetrachloride system focused on testing a model of molecularly sharp interfaces broadened by capillary wave surface fluctuations. Direct observations supported this picture, and a series of calculations with successively larger interfacial areas established its thermodynamic consistency.

2.4. Recent Experimental Probes of Aqueous Interface Structure

The picture that emerges from the modeling work is that aqueous interfaces with nonpolar liquids are molecularly sharp with fewer but more efficiently made water−water H-bonds. Moreover, distributions of preferred orientations of interfacial water molecules are broad and unexpectedly subtle. The calculations that lead to this picture are in good agreement with thermodynamic properties of interfacial systems. It is not surprising, however, that securing direct experimental structural confirmations has been a challenge.

2.4.1. Surface Nonlinear Optics Experiments

Surface nonlinear optics experiments, second harmonic generation, and sum frequency generation have been especially relevant. There has been lots of activity, progress, and current reviews of this work.[145−152] We refer the reader to those reviews for the big picture and the numerous technical details. Here we review activities directly pertinent to our understanding of hydrophobic effects.

There have been several direct efforts to interpret the surface nonlinear optics experiments in terms of the pictures obtained from modeling and simulation calculations.[117,153−155] Those efforts have been fairly successful and have provided important support of the picture described here. Nevertheless, experimental results are piling up at an accelerating pace, and in recent years it has not been always clear whether new structural interpretations are required;[156−160] less elliptically, there are apparent conflicts between the pictures above and recent experimental results. One puzzle is associated with "...weak hydrogen bonding and strong orientation effects"[158] for water molecules in the water−carbon tetrachloride interface. That sounds almost antithetical to the picture above which might be similarly paraphrased as strong hydrogen bonding and statistical orientation effects. The former view was developed from sum frequency generation studies that suggested important differences in the water molecule vibrational spectra for interfacial water in water liquid−vapor, water−*n*-hexane, and water−carbon tetrachloride interfaces. There are several background points to be made. The tensions of water−hydrocarbon liquid and water−carbon tetrachloride interfaces are significantly lower than the tension of the water liquid−vapor interface. These liquid−liquid interfaces would still be considered 'high tension' interfaces, however. These differences are typically attributed to water−hydrocarbon molecule interactions generically of attractive London dispersion type. A second point is that these interfaces are electrically asymmetric, and for that reason molecular polarizability may play a different role for the interfaces than it does for bulk liquids. Nevertheless, direct theoretical tests of the role of molecular polarizability in modeling the water liquid−vapor interface has suggested that it is a quantitative issue,[118] secondary to qualitative molecular pictures of these interfaces. Molecular calculations on the water−carbon tetrachloride interface using current force fields without molecular polarizability produce encouraging accuracy against experimental surface tension and indicate a molecularly sharp interface.[144] Molecular calculations with and without polarization have been compared. However, merely excluding induced dipoles does change the densities of the coexisting bulk phases and that complicates the desired comparison.[143] It is clear that more work is required to reconcile these points and the vibrational spectroscopy.

2.4.2. X-ray Reflectivity

Recent X-ray reflectivity studies also suggest that our description of these interfaces is not yet final.[161,162] This work concluded that a molecular 'intrinsic width' contribution must supplement a capillary wave width for water−alkane interfaces through C22 alkanes, and this intrinsic width increases with molecular size through the dodecane case. More disturbingly, the measured values of the interfacial widths are in disagreement with the results of computer simulations.[42,140−142] The reason for this disagreement is currently not understood.

2.5. Water–Membrane Interfaces

Considerations of interfaces between water and lipid bilayers introduce a new structural element that is not present in biphasic systems involving water and organic liquids. Water is no longer directly in contact with a nonpolar phase but instead is separated by strongly hydrophilic headgroups from the hydrophobic core of the membrane formed by hydrocarbon tails of lipids.

In the past decade, molecular-level computer simulation of water−membrane systems has become a mature field. During this period there have been numerous computational studies of bilayers made of glycolipids,[163] phospholipids with saturated or unsaturated chains,[164−185] and their mixtures with other membrane components.[186−190] Several reviews summarized some of this work.[165,191−194] The most recent calculations were able to reproduce an impressive range of structural and dynamic properties of membranes measured in X-ray scattering, neutron scattering, NMR, and infrared spectroscopy experiments.[195] In addition, computer simulations provided information that is difficult to obtain experimentally. We do not intend to review that work here. Instead, we just summarize a few of the more salient results relevant to the discussion of the hydrophobic effect.

In contrast to water−oil systems, interfaces between water and lipid bilayers are not sharp on the molecular scale. Water extensively penetrates the headgroup region hydrating phosphate, choline, and glycerol moieties. Figure 3 clearly illustrates this difference. The degree of hydration depends on the simulated hydration level of the bilayer. For example, the recent simulations of dioleoylphosphatidylcholine (DOPC) bilayer at different hydration levels[184] revealed that the number of water molecules in the headgroup hydration shell initially increases with the level of hydration but reaches saturation at 12 water molecules per lipid. This result is in agreement with the number inferred from X-ray scattering experiments.[196]

One consequence of water penetration into the headgroups is that the interfacial region is densely occupied whereas aqueous liquid−liquid interfaces behave, in some respects, as low-density regions. This is shown in Figure 4. Furthermore, orientational preferences of water molecules found at water surfaces in contact with hard hydrophobic walls, gas phase, or nonpolar liquids no longer hold. Orientations of water molecules near lipid bilayers are primarily determined by strong electrostatic interactions between water and charged or polar headgroup fragments.

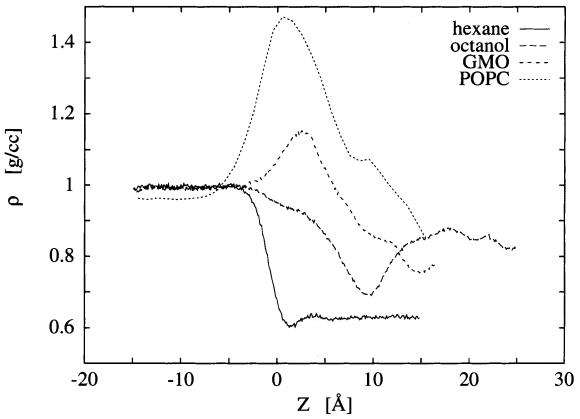

Figure 4. Mass density profiles at the water−hexane, water−octanol, water−glycerol l-monooleate (GMO), and water−l-palmitoyl-2-oleoyl-*sn*-glycero-3-phosphatidylcholine (POPC) interfaces. Water is located on the left side, and $z = 0$ corresponds to the equimolar surface of water. Mass density at the interface is the lowest for the water−hexane system and the highest for the water−POPC system.

Despite these differences there are also similarities between water−membrane systems and biphases containing water and an organic liquid. The most important one is that in both instances the polar and nonpolar phases remain separated. Indeed, as shown in Figure 3, water penetration into the hydrophobic core of the membrane was found to be small in almost all simulations. This separation forms the basis for a host of interfacial phenomena that are similar in both systems and is the reason a biphasic system can be, in some cases, an acceptable mimic of a water−membrane system. Another similarity among these two systems is that both are flexible. In fact, it was shown in computer simulations that water−membrane interfaces undergo capillary wave fluctuations in much the same way as water surfaces.[144,163,179,197,198]

Water−membrane interfaces do, however, represent the character of water at biologically relevant surfaces better than biphasic systems. Most biological macromolecules or subcellular structures expose hydrophilic groups to water even if their core is hydrophobic.

3. Solute Molecules at Aqueous Interfaces

The hydrophobic effect at aqueous interfaces influences not only the structure of the surface water but also the behavior of a wide variety of solutes in the interfacial region. Its role in modulating interfacial behavior did not receive much attention in early studies of hydrophobicity-driven phenomena even though this behavior is important in many areas of chemistry, biology, and pharmacology. Only in the last several years was this line of research vigorously pursued, mostly through computer simulations. The results of these simulations considerably improved our understanding of experimentally observed behaviors and, in some instances, led to the discovery

of new behaviors, subsequently confirmed in the laboratory. Specifically, the density distributions of many solutes, obtained from the profiles of the excess chemical potential (see eq 2), change across the interface in ways difficult to anticipate from their properties in bulk phases. The main feature of this interfacial behavior is the tendency to accumulate at the interface. Furthermore, flexible solutes that contain both polar and nonpolar groups often tend to be more rigid and ordered at the interface than in the aqueous solution. In particular, a host of peptides and small proteins with a favorable sequence of hydrophilic and hydrophobic residues adopt ordered structures at the interfaces even though they exist in water as random coils. This reinforces the view that the hydrophobic effect plays a fundamental role in organizing both animate and inanimate matter.

3.1. Interfacial Activity and Orientational Preferences of Small Solutes

In this section we consider the interfacial behavior of three types of solutes: amphiphilic, hydrophobic (nonpolar), and hydrophilic (polar).

3.1.1. Simple Amphiphilic Molecules at Interfaces

The simplest solutes to consider at the interface between water and nonpolar media are amphiphiles. Once dissolved in a bulk phase at low concentrations, these molecules adsorb at the interface with their hydrophilic part immersed in water and their hydrophobic part exposed to the nonpolar medium. This behavior is in line with our basic notion of the hydrophobic effect. However, even in this simple case, hydrophobic effects might manifest themselves differently than in the bulk water. One such example was shown in a molecular dynamics simulation of *p*-*n*-pentylphenol at the water−vapor interface.[199] In this simulation it was demonstrated that both the orientational and conformational preferences of the alkyl chain depended on the position of the phenyl ring with respect to the water surface. When the polar phenol headgroup was located at the water surface, the alkyl chain was partially folded and adopted an orientation nearly parallel to the surface, so that it could interact with water through dispersion forces. However, as the polar headgroup was progressively moved into the liquid, the orientation and conformation of the chain were changed according to a simple principle—maximization of the hydrophobic portion of the molecule removed from water. This can be accomplished by progressively aligning the molecule with the surface normal and adopting extended conformations of the chain. When the center of mass of the phenol ring was located 8 Å into the liquid from the equimolar surface of water, the chain was nearly perpendicular to the surface and all its torsional angles were preferentially trans. Such behavior contrasts sharply with the preferences observed in the bulk aqueous solution. There the hydrophobic effect drives the chain into folded states, presumably to minimize the work needed to create a cavity in water that can accommodate the solute. Such preferences were observed but only when the phenol ring was moved into the liquid sufficiently deep that no portion of the molecule could be removed from water for any orientation or conformation.

3.1.2. Distribution of Hydrophobic Species through Interfaces

Simple considerations based on our understanding of the hydrophobic effect lead us to an expectation that equilibrium concentrations of nonpolar solutes should increase from water to the nonpolar phase across the interfacial region. Calculations of the excess chemical potential through interfaces between water and nonpolar liquids[143,200−204] and membranes[200,204−207] performed for several small, hydrophobic solutes at infinite dilution as well as simulations of such solutes at finite concentrations at the water−membrane interface[203,208−210] confirm these expectations. However, when a solute molecule is polar but not amphiphilic, its interfacial behavior might not be as easy to anticipate.

3.1.3. Activity of Polar Molecules at Interfaces between Water and Organic Liquids or Membranes

Computer simulations show that a broad range of solutes, differing in size and chemical structure, tend to accumulate at the interface. The simulations also provide a conceptual basis for understanding this phenomenon. This is accomplished by appealing to the potential distribution theorem discussed in section 1.2.2. Then simulations are designed so that eq 2 can be directly applied to calculate changes in the excess chemical potential. Conceptually, the central underlying idea is to consider these changes as a sum of two contributions, which represent the work expended quasi-statically to create a cavity sufficiently large to accommodate a solute and the free energy changes caused by solute−solvent interactions and the accompanying solvent reorganization.[200,204,206] Changes in the first term—the excess chemical potential of an idealized, hard-core molecule with size and shape corresponding to the solute of interest—are directly related to the hydrophobic effect. The second term is primarily due to changes in electrostatic interactions.

This perspective on solvation is hardly new. In fact, accurate and efficient calculations of the first term were at the center of several theories of hydrophobic hydration, including the scaled particle theory[211] and, more recently, the information theory of the hydrophobic effect.[39] However, this point of view appears to be particularly revealing in studies of interfacial solvation. Why this is the case can be simply explained in the example of a spherical, dipolar solute at the water−hexane interface. If the cavity is of atomic size, the reversible work of its insertion into the solvent can be readily calculated using the particle insertion method.[37,212] The electrostatic contribution to the chemical potential can be obtained simply from the knowledge of the instantaneous electric field at the center of the cavity.[200] The results are shown in Figure 5. In agreement with our view of the hydrophobic effect, the work needed to form a cavity in water is considerably larger than the work of forming a cavity in a nonpolar phase. This reflects the poor solubilities of nonpolar species—of which a

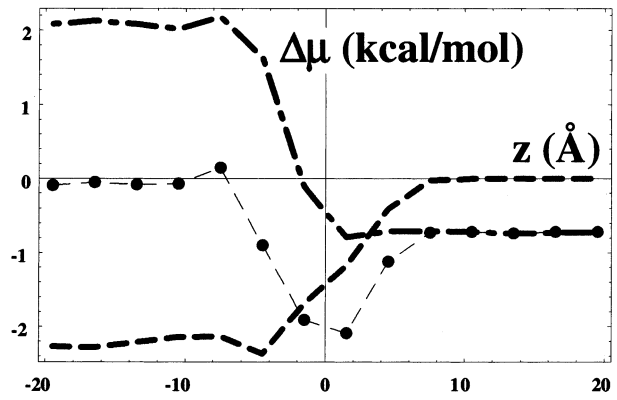

Figure 5. Free energy, the right-most term of eq 1, for positioning the carbon atom of CH_3F in the *n*-hexane−water interface (large dots joined by a thin dashed line). The free energy exhibits the minimum at $z = 0$, which is located at the equimolar surface of water. The liquid water is to the left and the hexane phase is to the right. The minimum, which reflect interfacial activity of the solute arises from combining two contributions, the hydrophobic contribution (the dot-dash curve) and the electrostatic contribution (the dashed curve, lowest on the left).

cavity is an idealized example—in water compared to other organic liquids. The small interfacial minimum can be ascribed to weak interactions between water and oil. The densities of both liquids at the interface are considerably reduced compared to the bulk densities (see Figure 3), and there is almost no molecular-scale interpenetration between the two phases in contact.[136,144,213] The slight degree of interpenetration suggests that the properties of water molecules at the interface with a nonpolar phase have this similarity to vapor contacts. In fact, the probability of finding a cavity of atomic or small molecular size at the interface is larger than in either of the bulk phases.[42] This can be taken as a moderate interpretation[8] of the recent 'drying' conceptualizations[50] of these interfaces.

In contrast to the hydrophobic contribution, the term due to electrostatic interactions increases almost linearly from its value in bulk water to zero in hexane over a distance of approximately 10 Å. The interfacial minimum in the total excess chemical potential reflects the balance between these two terms that change oppositely across the interface.[200,203,204,206,214] Within a fairly broad range, changes in the sizes of the cavity and the dipole moment influence only the depth of the minimum but do not qualitatively change the shape of the chemical potential profile.[200]

Qualitatively similar results, pointing to the interfacial activity of polar species, were obtained from molecular-level computer simulations of a variety of solutes at interfaces between water and hexane,[200,202,214] carbon tetrachloride,[143] octanol,[204] and several membrane-forming lipids, such as glycerol 1-monooleate (GMO),[200,201,203,204] 1-palmityol-2-oleoyl-*sn*-glycero-3-phosphatydylcholine (POPC),[204] dimyristoylphosphatydylcholine (DMPC),[207] and dipalmitoylphosphatydylcholine (DPPC).[210,215,216] The solutes under study ranged from simple, nearly spherical molecules such as fluorinated methanes,[200] chloroform,[143] and CO_2[207] to halothane,[210,215,216] ethers,[202,214] and halogenated butanes and cyclobutanes.[202,214] A recent study[217] of 'the TFE effect' of trifluoroethanol in promoting helix formation in polypeptides suggests some surface activity for TFE also.

Although the tendency to accumulate near the interface appears to be common, there are differences between the behavior of solutes at water interfaces with oil and phospholipids (and, to a lesser extent, octanol and GMO). The interactions between water and the polar headgroups of membrane-forming amphiphilic molecules are markedly stronger than the water−hexane interactions. Furthermore, in contrast to the water−hexane system, in which there is no molecular-level interpenetration between the phases in contact, water significantly penetrates the headgroup region. In this case, there is no increase in available volume at the interface. A "vapor-like" picture of the interfacial water does not apply to interfaces with phases formed by molecules which possess polar groups, such as octanol and lipids. Similarly, this picture is unlikely to apply to water at surfaces of globular proteins, which have a large number of hydrophilic residues exposed to the solvent. At the water−membrane interface, the probability of inserting a cavity does not increase compared to bulk phases. In fact, due to the increased atomic density (see Figure 4), the chemical potential of cavity insertion in the phospholipid headgroup region exhibits a maximum.[204] This, in turn, may lead to expulsion of solutes from this region.[207,216] Instead, solute molecules are predominantly located in the upper part of the lipid tails, adjacent to the headgroups. In this more rigid and less densely packed region, cavity insertion is more probable than at the interface.[200,205] These preferences are strong. For example, 95% of halothane molecules placed in the DPPC membrane were located in this region and only 5% occupied the core of the bilayer.[216] This was in sharp contrast to a hydrophobic 1,2-dichlorohexafluorocyclobutane, which was broadly distributed across the bilayer with preference toward its center.[210] A similar result was obtained for a hydrophilic/hydrophobic pair of solutes, 1,1,2-trifluoroethane and perfluoroethane, in the water−GMO system.[201]

3.1.4. Biological Significance of Solute Distributions in Water–Membrane Systems

Much of the motivation to study small solutes at aqueous interfaces arose from a possible connection between the interfacial activity of these solutes and their ability to function as anesthetics. In particular, it was shown that anesthetics are located in the lipid bilayer near the headgroup region whereas structurally related nonanesthetics (nonimmobilizers) partition to the center of the bilayer.[201,203,210,218] Although the mechanism of anesthetic action remains unknown, the results of these studies might be biologically relevant, especially to regulation of membrane channels and receptors. For example, it was shown that halothane induces lateral expansion of the DPPC membrane accompanied by contraction the bilayer thickness.[210,215,216] Furthermore, structural

changes in lipids induced by the anesthetic caused significant modifications of the electric properties of the bilayer, in particular a shift and broadening of the choline headgroup dipole orientation distribution. These findings are each related to a hypotheses that links interfacial concentrations of solutes, such as anesthetics, to receptor action. According to one hypothesis, incorporation of solutes into the interfacial region results in large, differential lateral stresses, which can affect receptors and open or close transmembrane channels.[219−223] Another hypothesis posits that changes in electrostatic properties at the surface of the membrane may modulate voltage-dependent conformational transitions in membrane receptor and, by doing so, regulate their activity.[224,225]

Until a few years ago, the interfacial activities of small, polar molecules and the connection with hydrophobic effects were not widely appreciated. Once computer simulations addressed this issue, experimental tests followed and confirmed the correctness of computational results. The NMR measurements of the distribution of solutes in water−phospholipid bilayer revealed that a slightly polar anesthetic 1-chloro-1,2,2-trifluorocyclobutane exhibits a preference for the membrane interface whereas a hydrophobic 1,2-dichlorohexafluorocyclobutane is mostly located in the hydrocarbon core of the membrane.[226,227] Furthermore, polar halothane, isoflurane, enflurane, and ethanol and strongly polarizable xenon also show affinity toward the interface.[228−230]

3.1.5. Orientations and Conformations of Amino Acids and Dipeptides at Aqueous Interfaces

An especially interesting class of small, electrically neutral solutes at interfaces is terminally blocked amino acids and dipeptides. Several of them were studied at the water−hexane[231] and the water−GMO interface.[232] All were found to be strongly interfacially active even if their side chains were purely hydrophobic (e.g., acyl chains). This is not surprising in view of the previous discussion; all amino acids contain polar C═O and N−H groups. The polarity of the side chain influenced the orientation at the interface, however. As expected, hydrophilic amino acids, such as glutamine, were oriented with their side chains immersed in water, whereas hydrophobic amino acids, such as leucine, adopted orientations that allowed the side chains to be buried in hexane.

The same tendency was observed for terminally blocked dipeptides, which were studied in bulk water, hexane, the gas phase, and the interfacial environment.[233] Compared to hexane and the gas phase and irrespective of the nature of the side chains, water drove all dipeptides toward compact conformations. This agrees with our expectations about the influence of hydrophobic effects and conformational equilibria. The effect noted here is nonspecific. At the interface, the preferred conformations of the peptide backbone corresponded to optimal interactions of the side chains with the media of similar polarity. Dipeptides containing one hydrophobic and one hydrophilic residue adopted an "amphipathic" $\alpha_R\beta$ orientation, whereas dipeptides made of two hydrophobic or two hydrophilic amino acids were oriented to maximize exposure of their side chains to hexane and water, respectively.

4. Peptides and Peptide Folding at Interfaces and insertion of Peptides into Membranes

The discussion of dipeptides at interfaces serves as an introduction to a subject of considerable biological importance: interactions of peptides and small proteins with water−membrane interfaces. The main theme here is that the hydrophobic effect in these environments is central for inducing ordered structures in a variety of proteins that are disordered in aqueous solution. Furthermore, the distribution of hydrophobic and hydrophilic side chains along these ordered structures influences the disposition of peptides (interfacial or transmembrane) and, ultimately, determines their cellular functions.

Many proteins that insert themselves into membranes are involved in such essential cellular functions as energy transduction, signal transmission, catalysis of some metabolites, and transport of nutrients, waste products, and ions.[234−237] Other peptides and proteins, including hormones, toxins, antibacterial agents, membrane fusion proteins, pulmonary surfactant proteins, and amyloid peptides, interact preferentially with membrane surfaces.[238−242] This distinction is somewhat blurred because at sufficiently high concentrations and/or in the presence of an electric field, many naturally occurring or synthetic peptides convert from a surface orientation to the transmembrane orientation.[243−247] Furthermore, these two types of proteins share many properties. They are usually disordered in water but fold into α-helices or, less often, β-sheets or β-turns upon contact with the membrane. Some membrane peptides and proteins contain mostly hydrophobic residues, whereas many others are built of periodically spaced polar and nonpolar amino acids.

The appropriate hydrophobic periodicity allows peptides to form an ordered structure in which polar and nonpolar residues are located at opposite faces. At the water−membrane interface, amphiphatic structures can readily adopt an orientation in which the hydrophilic face is buried in water while the hydrophobic face is exposed to the nonpolar environment formed by the hydrocarbon tails of the lipids. This match between the polarities of the peptide and its environment renders the amphiphatic structures particularly stable.

4.1. Interfacial Folding of Peptides and Protein Fragments

Early molecular-level computer simulations[248−250] were limited to trajectories just a few hundred picoseconds long. On that time scale, peptide structure does not change appreciably, as was indeed found in the simulations. However, even these early studies revealed a strong tendency of small peptides to adopt or retain amphiphatic structures at interfaces. They could correspond to either a parallel[250] or perpendicular[249] orientation with respect to the membrane surface. In particular, it was shown that a small, fusion-inhibiting peptide carbobenzoxy-D-

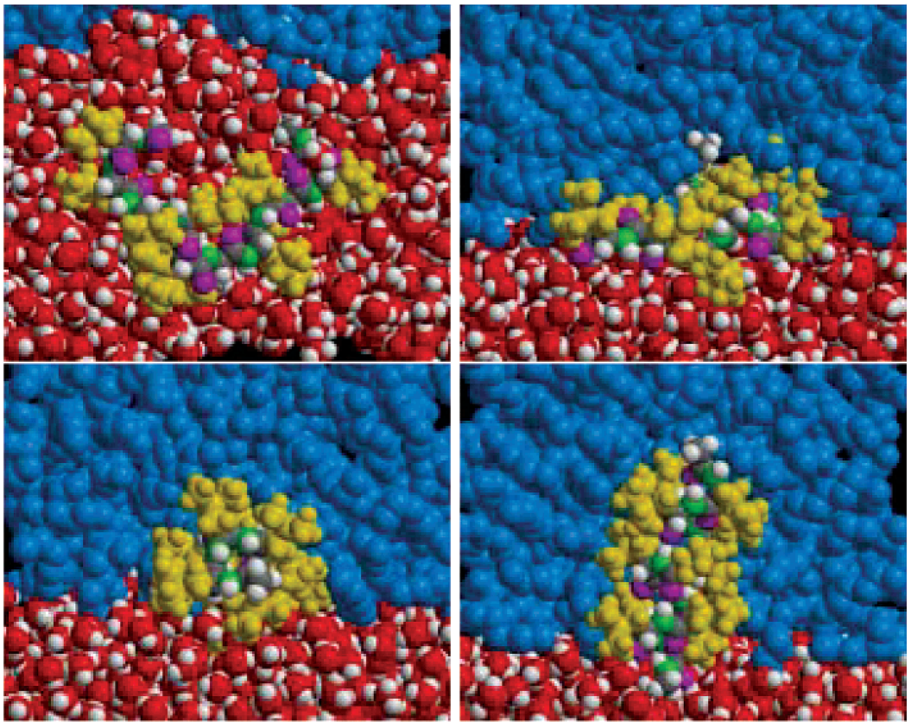

Figure 6. Undecamer of poly-L-leucine at the water−hexane interface. Oxygen and hydrogen atoms of water are red and white, respectively. Methyl and methylene groups of hexane are blue; all atoms in the peptide side chains are yellow. Carbon, nitrogen, and oxygen atoms of the peptide backbone are gray, green, and magenta, respectively. Starting with the upper left: the initial, disordered structure of the peptide on the water side of the interface, a partially folded, nascent helix at the interface after 21 ns, a completely folded helix located parallel to the interface (viewed along the helical axis), a helix with the N-terminus inserted into hexane.

Phe-L-Phe-Gly inserts into a phospholipid bilayer in a way similar to the lipid molecules.[249] In this orientation, the C-terminus plays the role of the polar headgroup while the phenyl rings form the hydrophobic core.

Only recently have computational capabilities became sufficient to address more interesting issues such as the mechanism of interfacial folding and insertion into the membrane. The results are not only relevant to understanding the structure and function of membrane proteins but may also provide new insight into the mechanism of folding of water-soluble proteins.

In the first molecular-level study that explicitly addressed interfacial folding of proteins, a 50 ns trajectory was obtained for the undecamer of poly-L-leucine at the water−hexane interface.[251] The choice of a membrane-mimetic phase instead of a membrane was motivated by concerns that the slow relaxation of the collective motions of the bilayer-forming phospholipid molecules could markedly impede peptide motion. This concern was confirmed in the recent simulations of alamethicin in a water−membrane system.[252] The polyleucine peptide, initially placed in the aqueous phase as a random coil (see the first panel in Figure 6), rapidly translocated to the interface, presumably because in this environment nonpolar leucine residues could be, at least in part, removed from water. Once at the interface, the peptide folded into a helix in 36 ns (see the lower left panel in Figure 6). During this process, some polar groups in the backbone became dehydrated, which facilitated the formation of intramolecular hydrogen bonds along the backbone. The resulting structure of the peptide became more hydrophobic and partitioned further into the hexane phase. This, in turn, created a favorable environment for the emergence of additional, structure-forming intramolecular hydrogen bonds. Folding, however, was not sequential but instead was highly dynamic and involved multiple cases of intermittent breaking and reforming of hydrogen bonds (see the upper right panel in Figure 6). Even the folded structure was dynamic, interconverting between an α- and 3_{10}-helix.

The role of the interface in mediating the segregation of hydrophobic and hydrophilic side chains into different environments and, by doing so, inducing ordered peptide structures was further investigated in studies of an undecamer built of L-leucine and L-glutamine, LQQLLQQLLQL, at the water−hexane interface.[253] The peptide is amphiphatic as an α-helix but not as a β-strand. Thus, it might be expected that the peptide should rapidly fold to an α-helix and remain in this highly stable structure. These expectations were based on experimental studies on similar, short peptides at aqueous interfaces.[245,254−258] Here, particularly relevant are results for synthetic peptides composed of leucine and serine that have the same distribution of polar and nonpolar residues as the undecamer.[259,260] The expectations were further supported by simulation of the undecamer placed at the interface in the α-helical conformation.[233] This conformation remained perfectly stable during a molecular dynamics trajectory 11.3 ns long. However, the LQQLLQQLLQL undecamer itself has not been studied experimentally, and no direct evi-

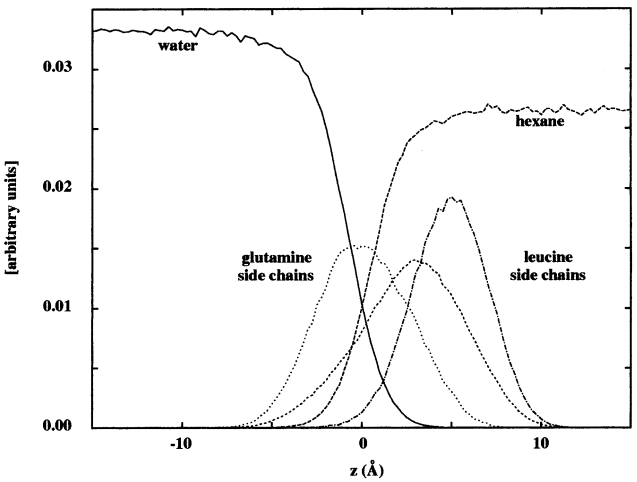

Figure 7. Density profiles of the terminally blocked leucine(L)/glutamine(Q) undecapeptide, LQQLLQQLLQL, at the water−hexane interface: leucine side chains (- · -), glutamine side chains (···), and peptide backbone (- - -). Water (—) and hexane (— — —) density profiles are also included. Hydrophobic leucine residues are buried in hexane, while glutamine side chains are located on the water side of the peptide.

dence exists demonstrating its helicity in an interfacial environment. When the peptide was assigned the β-strand conformation, a 160 ns trajectory was insufficient to observe complete refolding to the α-helix. Initially, the peptide rapidly underwent several conformational transitions to adopt a nearby amphiphatic structure. In the remaining time, several more rotations around the ϕ and ψ angles in the peptide backbone were observed. In all cases, the peptide structures were amphiphatic, as illustrated in Figure 7. This led to the formation of a few intramolecular hydrogen bonds along the backbone characteristic of a helical structure, but the peptide did not fully fold. The results indicate that folding pathways at aqueous interfaces are limited by the requirement that intermediate structures be amphiphatic whenever possible. Interfacial folding of peptides containing both hydrophobic and hydrophilic residues appears to be slower that folding of purely hydrophobic peptides because transitions between consecutive amphiphatic structures may require surmounting substantial free energy barriers associated with dehydration of hydrophilic side chains. Furthermore, folding may be impeded by bottlenecks resulting from the presence of nonamphipathic structures along the folding pathway. Similar conclusions were reached from simulations of the heptamer LQQLLQL at the water−air interface.[233]

Results of recent, extensive simulations of protein folding at the water−hexane interface[261] support the findings of the earlier studies on model peptides, confirming the role of the hydrophobic effect in inducing ordered structures. In these simulations it was shown that a fungal protein, hydrophobin SC3, truncated to 86 residues, folds at the interface to an elongated planar structure with extensive β-sheet elements in approximately 100 ns. By comparison, simulations of the same protein in bulk water and hexane yielded mainly disordered globular protein. In agreement with experimental data, SC3 was found to be strongly interfacially active. The authors infer that "the strong electrostatic interaction between the water molecules, leading to a high free energy cost for cavity formation, is a major factor contributing to the free energy minimum". This is essentially the same interpretation as that given to explain interfacial activity of small solutes and terminally blocked amino acids.[200,203,231]

Once the protein reached the interface, almost all of its conformations were amphipathic. This further supports the idea that interfacial folding proceeds through a series of amphipathic intermediates. Since the primary sequence does not consist of alternating hydrophilic and hydrophobic residues, which are necessary for the formation of an amphipatic β-strand, some mismatches between hydrophobicity of side chains and their environment were observed once β-sheets were formed toward the end of the simulation. However, their number was small compared to those that would have existed in a random structure. Furthermore, these mismatches might be functionally important to drive aggregation of individual hydrophobin molecules into rodlets.

A strong tendency to retain amphiphatic structure at the interface was also observed in simulations of an 11-residue neuropeptide, substance P, in a biphasic water−carbon tetrachloride system[262] and at the surface of sodium dodecyl sulfate micelles.[262] The structure of this peptide is neither a pure α-helix nor a β-strand but instead contains two type I β-turns. This structure was determined from NMR and CD studies of substance P in lipid environments[263] and is consistent with the recent results of neutron diffraction studies on the interaction of substance P with phospholipid bilayers.[264] The peptide, initially placed in the conformation similar to the one reported by Keire and Fletcher,[263] executed concerted conformational transitions during hundreds of picoseconds while it maintained largely amphiphatic structures. Hydrophobic residues proline, phenylalanine, leucine, and methionine were mostly removed from water and buried in the nonpolar phase.

Another factor that influences conformations and folding of proteins at aqueous interfaces is the structure of interfacial water. This was revealed in a 1.5 ns molecular dynamics study of the N-terminal domain of apolipoprotein E at the interface between water and carbon tetrachloride represented as a Lennard−Jones liquid.[265] As has already been discussed (see Figure 2 and sections 2.1 and 2.2), interfacial water molecules tend to have one unsatisfied hydrogen-bonding site. These sites are available for efficient bonding with the protein solute. This increased ability to form water−protein interactions allows for water penetration into the tight four-helical protein bundle that exists in water. The internal hydration of the protein, in turn, may lead to the decrease in the energy barriers that separate this structure from a more open conformation bound to the lipid. A strong tendency to keep the protein backbone either well solvated by water or hydrogen bonded was also observed in simulations of substance P.[262]

The role of an interfacial environment in inducing protein structures was further underscored in extended simulations of polyalanine and alamethicine, which demonstrated that the α-helical conformations of these two peptides are stable at the water−hexane interface but they partially unfold in multiple simulations in water.[252]

In summary, the coexistence of two phases with different polarity and the tendency to remove hydrophobic side chains from aqueous environment provides a driving force that enables or enhances secondary structure formation for proteins that interact with or incorporate into membranes. It is less clear whether interfaces also form a favorable environment for folding of globular proteins. In fact, adsorption of proteins to interfaces may cause a loss of secondary or tertiary structure. This may be associated with an increase of entropy of the protein due to its partial immobilization at the interface or a mismatch between polarities of side chains and their environment in the folded structure.

4.2. Hydrophobic Effects and Insertion of Peptides into Membranes

A protein adsorbed at a water−membrane interface may either remain in this location or insert into the membrane. It might be expected that the transmembrane orientations would be preferred for hydrophobic peptides. In agreement with this expectation, it was found that polyalanine initially placed as a transmembrane α-helix in a phospholipid bilayer[252,266] or octane lamella[252] remains folded and retains its orientation during the course of the simulations. Simulations of mellitin at the water−membrane interface[267] further support this view. Mellitin consists of two short α-helical portions, of which one is hydrophobic and the other is hydrophilic. The peptide was initially placed parallel to the interface, but in less than 500 ps its hydrophobic portion protruded into the hydrophobic tail region of the membrane. The picture emerging from simulations of a strongly hydrophobic undecamer of poly-L-leucine at the water−hexane interface[251] is somewhat more complicated. The most favorable orientation of the peptide was parallel to the interface. The free energy of perpendicular orientations with the N- or C-terminus buried in hexane was, respectively, 4 and 12 kcal/mol less favorable. The latter orientation is shown in the bottom right panel of Figure 6. This conclusion is in qualitative agreement with calculations of the free energy of transferring an α-helix from water to a lipid bilayer based on a continuum dielectric model.[268] These calculations showed that parallel and perpendicular orientations are nearly equally probable. It should be noted, however, that the undecamer was too short to span the hexane lamella, so that both hydrophilic termini would be exposed to water.

For amphiphatic peptides, adsorption at the interface should be strongly favored over transmembrane orientation. Not surprisingly, spontaneous insertion of amphiphatic peptides into a membrane have not been observed in molecular-level computer simulations. In contrast, substance P peptide, initially placed in an orientation perpendicular to the water−CCl_4 interface, converted to a nearly parallel orientation in approximately 250 ps.[262] A similar result was obtained for an adrenocorticotropin hormone fragment in a hydrated dodecylphosphocholine micelle.[269] However, the insertion process most likely does occur. In the prevailing model of folding transmembrane proteins[270−273] it is assumed that initially formed elements of the secondary structure incorporate into the membrane before they associate to form a fully functional protein. The same mechanism is assumed in the aggregation of multimeric ion channels. Favorable free energy of helix association balances out unfavorable free energy of helix insertion into the membrane leading to stable transmembrane protein complexes (but not individual helices). Even in the examples discussed here the results are ambiguous. Specifically, neutron diffraction data for substance P were interpreted in terms of an equilibrium between orientations of the peptide parallel and perpendicular to the bilayer.[264]

In many instances the insertion of an amphiphatic peptide into the membrane is facilitated by electric field. This process was successfully simulated for alamethicin in the water−octane system.[252] At field strengths of 0.33 V/nm and higher the peptide became inserted into octane in less than 100 ns. However, insertion into phospholipid bilayer was not observed during a 10 ns simulation.[252] Voltage-induced insertion of an α-helix was also observed in simulations of endotoxins at a simplified water−membrane interface.[246] However, not all amphiphatic peptides seem to insert into membranes, even in the presence of electric field. One such case, investigated in molecular dynamics simulations, is the mammalian antibacterial peptide cecropin P1.[242]

Specific interactions between water and different groups in protein mediate its insertion into membranes in several ways. First, in several simulations it was noted that insertion of the N-terminus of a peptide appears to be more likely that insertion of the C-terminus.[251,252,267,274] The same effect was also observed experimentally.[275] The most likely explanation of this preference[251,268] is that the peptide backbone at the C-terminus but not at the N-terminus contains unsatisfied hydrogen-bonding sites. Partition of the C-terminus into the membrane would have required the dehydration of these sites, which strongly interact with water but are unable to participate in intramolecular hydrogen bonds. Second, water bound to hydrophilic groups in proteins is capable of penetrating deep into the hydrophobic core of the membrane. Simulations of dynorphin,[274] melittin,[267] and a transmembrane segment of the $5HT_{2a}$ receptor[276] provide relevant examples. Finally, in several instances it was observed that the nonpolar part of a lysine residue was surrounded by hydrocarbon chains while its positively charged nitrogen atom was solvated by deeply penetrating water molecules.[262,267,274] This "snorkel effect" was proposed by Segrest et al.[277] to explain the amphiphatic character of lysine side chains.

5. Conclusions

The areas reviewed here are subjects of very active research motivated to a large extent by their wide importance in biotechnology and nanotechnology. [Though we do not review those fields here, references[278−281] give current examples that involve hydrophobic effects.] Hydrophobic effects clearly play a fundamental role in determining structures of macromolecules and in driving their environment-mediated self-assembly into higher order structures. In most cases these effects have not been neatly disentangled from other contributing effects, such as electrostatic or specific interactions. These factors, in combination with the explosive growth in capabilities of molecular simulations, make it nearly impossible to provide an exhaustive review of all the topics related to the issues addressed here. We make no claims that this review does that. Nevertheless, the body of work reviewed here permits several foundational conclusions.

Current simulation models and calculations give a remarkably accurate description of the properties of liquid water in coexistence with its vapor, particularly in view of the simplicity of the molecular models. These properties include the liquid−vapor coexistence curve, the dielectric constant of the liquid in coexistence with its vapor, and the surface tension over a wide temperature range. The most recent experiments (sum frequency generation and X-ray reflectivity) suggest that, at a high resolution, current descriptions of simple water−oil interfaces are not final. Nevertheless, the indications are that this situation is not a substantial limitation for calculations dealing with interfaces of biophysical interest.

The concentration, structuring, and orientation of amphiphilic solutes at aqueous interfaces is a dominating and conceptually clear aspect of hydrophobic effects in these settings. These effects are simpler than the temperature subtleties of hydrophobic phenomena in bulk phases.

This suggests the hypothesis that when the characteristic hydrophobic temperature dependences are observed for interfacial or macromolecule settings, these are primarily due to thermodynamic reference to disassembled, dispersed, or unfolded states. This suggestion is tentative and thus requires further investigation.

Although interfaces of liquid water with simple hydrophobic phases and with biophysical surfaces such as bilayer membranes have some common features, they are, in many other respects, qualitatively different. Hydrocarbon liquid−water interfaces are molecularly sharp with subtle orientational effects. Fluctuations of these interfaces provide easy access for a wide variety of interfacially active species. Interfaces saturated with surfactants are much broader with compositional heterogeneity as a dominating factor. As a consequence, orientational distributions and density profiles of water molecules at these interfaces lead to electrical asymmetry and distributions of free volume that are qualitatively different from oil−water or water−rigid wall interfaces. These differences are likely to extend to the structure and properties of interfaces between water and macromolecules, such as proteins vs carbon nanotubes.

6. Acknowledgment

This work was supported by the NASA Exobiology Program and the U.S. Department of Energy under contract W-7405-ENG-36 under the LDRD program at Los Alamos: LA-UR-02-1424.

7. References

(1) Dill, K. A. *Biochemistry* **1990**, *29*, 7133−7155.
(2) Tanford, C. *Protein Sci.* **1997**, *6*, 1358−1366.
(3) Tanford, C. *Science* **1978**, *200*, 1012−1018.
(4) Pohorille, A.; Wilson, M. A. *Origins Life Evol. Biosphere* **1995**, *25*, 21−46.
(5) Pohorille, A.; Chipot, C.; New, M.; Wilson, M. A. Molecular Modeling of Protocellular Functions. In *Pacific Symposium on Biocomputing '96*; Hunter, L., Klein, T., Eds.; World Scientific: Singapore, 1996.
(6) Segre, D.; Lancet, D. *EMBO Rep.* **2000**, *1*, 217−222.
(7) Blokzijl, W.; Engberts, J. B. F. N. *Angew. Chem., Int. Ed. Engl.* **1993**, *32*, 1545−1579.
(8) Pratt, L. R. *Annu. Rev. Phys. Chem.* **2002**, *53*, 409−436.
(9) Israelachvili, J.; Adams, G. *J. Chem. Soc.. Faraday Trans. I* **1978**, *74*, 975.
(10) Parsegian, V.; Rand, R.; Rau, D. *Proc. Natl. Acad. Sci. U.S.A.* **2000**, *97*, 3987−3992.
(11) Dill, K. A. *Biochemistry* **1990**, *29*, 7133−7155.
(12) Franks, F. *Water: A Comprehensive Treatise*; Plenum: New York, 1973; Vol. 2, Chapter 1, pp 1−54.
(13) Tanford, C. *The Hydrophobic Effect*: *Formation of Micelles and Biological Membranes*, 2nd ed.; John Wiley & Sons: New York, 1980.
(14) Mirejovsky, D.; Arnett, E. *J. Am. Chem. Soc.* **1983**, *105*, 1112−1117.
(15) Muller, N. *Acc. Chem. Res.* **1990**, *23*, 23−28.
(16) Spolar, R. S.; Ha, J. H.; Record, M. T. *Proc. Natl. Acad. Sci. U.S.A.* **1989**, *86*, 8382−8385.
(17) Livingstone, J. R.; Spolar, R. S.; Record, M. T. *Biochemistry* **1991**, *30*, 4237−4244.
(18) Urry, D. *Trends Biotechnol.* **1999**, 249−257.
(19) Li, B.; Alonso, D. O. V.; Daggett, V. *J. Mol. Biol.* **2001**, *305*, 581−592.
(20) Privalov, P. L. *Crit. Rev. Biochem. Mol. Biol.* **1990**, *25*, 281−305.
(21) Sterner, R.; Liebl, W. *Crit. Rev. Biochem. Mol. Biol.* **2001**, *36*, 39−106.
(22) Franks, F. *Faraday Symp. Chem. Soc.* **1982**, *17*, 7.
(23) Kauzmann, W. *Adv. Protein Chem.* **1959**, *14*, 1−63.
(24) Eisenberg, D.; Kauzmann, W. *The Structure and Properties of Water*; Oxford University Press: New York, 1969.
(25) Robinson, G. W.; Zhu, S.-B.; Singh, S.; Evans, M. W. *Water in Biology, Chemistry, and Physics*; World Scientific: Singapore, 1996.
(26) Rashin, A. A.; Bukatin, M. A. *J. Phys. Chem.* **1991**, *95*, 2942−2944.
(27) Rashin, A. A. *Prog. Biophys. Mol. Biol.* **1993**, *60*, 73−200.
(28) Rashin, A. A.; Bukatin, M. A. *J. Phys. Chem.* **1994**, *98*, 386-389.
(29) Sitkoff, D.; Sharp, K.; Honig, B. *J. Phys. Chem.* **1994**, *98*, 1978−1988.
(30) Marrone, T. J.; Gilson, M.; McCammon, J. *J. Phys. Chem.* **1996**, *100*, 1439−1441.
(31) Sharp, K. A.; Nicholls, A.; Fine, R. F.; Honig, B. *Science* **1991**, *252*, 106−109.
(32) Sitkoff, D.; Sharp, K. A.; Honig, B. *Biophys. Chem.* **1994**, *51*, 397−409.
(33) Hodes, Z. I.; Nemethy, G.; Scheraga, H. A. *Biopolymers* **1979**, *18*, 1611−1634.
(34) Kang, Y. K.; Nemethy, G.; Scheraga, H. A. *J. Phys. Chem.* **1987**, *91*, 4105−4109.
(35) Eisenhaber, F. *Perspect. Drug Discovery Des.* **1999**, *17*, 27−42.
(36) Hummer, G.; Garde, S.; Garcia, A. E.; Pratt, L. R. *Chem. Phys.* **2000**, *258*, 349−370.
(37) Widom, B. *J. Phys. Chem.* **1982**, *86*, 869−872.
(38) Paulaitis, M. E.; Pratt, L. R. *Adv. Prot. Chem.* **2002**, *60*, 283−310.
(39) Hummer, G.; Garde, S.; Garcia, A. E.; Pohorille, A.; Pratt, L. R. *Proc. Natl. Acad. Sci. U.S.A.* **1996**, *93*, 8951−8955.
(40) Pratt, L. R. Oil and Water Don't Mix. In *CLS Division 1991 Annual Review*; National Technical Information Service U.S. Department of Commerce: 5285 Port Royal Rd., Springfield, VA 22161, 1991.

(41) Pratt, L. R.; Pohorille, A. Hydrophobic effects from cavity statistics. In *Proceedings of the EBSA 1992 International Workshop on Water-Biomolecule Interactions*; Palma, M. U., Palma-Vittorelli, M. B., Parak, F., Eds.; Societa Italiana de Fisica: Bologna, 1993.
(42) Pohorille, A.; Wilson, M. *A. J. Mol. Struct.* (*THEOCHEM*) **1993**, *284*, 271−298.
(43) Siebert, X.; Hummer, G. *Biochemistry* **2002**, *41*, 2956−2961.
(44) Garde, S.; Hummer, G.; Garcia, A. E.; Paulaitis, M. E.; Pratt, L. R. *Phys. Rev. Lett.* **1996**, *77*, 4966−4968.
(45) Pohorille, A.; Pratt, L. R. *J. Am. Chem. Soc.* **1990**, *112*, 5066−5074.
(46) Pratt, L. R.; Pohorille, A. *Proc. Natl. Acad. Sci. U.S.A.* **1992**, *89*, 2995−2999.
(47) Hummer, G.; Garde, S.; Garcia, A. E.; Paulaitis, M. E.; Pratt, L. R. *J. Phys. Chem. B* **1998**, *102*, 10469−10482.
(48) Pohorille, A. *Pol. J. Chem.* **1998**, *72*, 1680−1690.
(49) Richards, F. M. *Sci. Am.* **1991**, *264*, 54.
(50) Lum, K.; Chandler, D.; Weeks, J. *D. J. Phys. Chem. B* **1999**, *103*, 4570−4577.
(51) Muller, E.; Hung, F.; Gubbins, K. *Langmuir* **2000**, *16*, 5418−5424.
(52) Cheng, Y.; Rossky, P. J. *Nature* **1998**, *392*, 696−699.
(53) Cheng, Y.; Rossky, P. J. *Biopolymers* **1999**, *50*, 742−750.
(54) Jonsson, B. *Chem. Phys. Lett.* **1981**, *82*, 520−525.
(55) Christou, N. I.; Whitehouse, J. S.; Nicholson, D.; Parsonage, N. G. *Faraday Symp. Chem. Soc.* **1981**, 139−149.
(56) Sonnenschein, R.; Heinzinger, K. *Chem. Phys. Lett.* **1983**, *102*, 550−554.
(57) Marchesi, M. *Chem. Phys. Lett.* **1983**, *97*, 224−230.
(58) Barabino, G.; Gavotti, C.; Marchesi, M. *Chem. Phys. Lett.* **1984**, *104*, 478−484.
(59) Lee, C. Y.; McCammon, J. A.; Rossky, P. J. *J. Chem. Phys.* **1984**, *80*, 4448−4455.
(60) Aloisi, G.; Guidelli, R.; Jackson, R. A. Clark, S. M.; Barnes, P. *J. Electroanal. Chem.* **1986**, *206*, 131−137.
(61) Luzar, A.; Bratko, D.; Blum, L. *J. Chem. Phys.* **1987**, *86*, 2955−2959.
(62) Valleau, J. P.; Gardner, A. A. *J. Chem. Phys.* **1987**, *86*, 4162−4170.
(63) Wallqvist, A.; Berne, B. J. *Chem. Phys. Lett.* **1988**, *145*, 26−32.
(64) Stillinger, F. H. *J. Solution Chem.* **1973**, *2*, 141−158.
(65) Wallqvist, A.; Berne, B. J. *J. Phys. Chem.* **1995**, *99*, 2885−2892.
(66) Chau, P.; Forester, T.; Smith, W. *Mol. Phys.* **1996**, *89*, 1033−1055.
(67) Ashbaugh, H. S.; Paulaitis, M. E. *J. Am. Chem. Soc.* **2001**, *123*, 10721−10728.
(68) Pratt, L. R.; Haan, S. W. *J. Chem. Phys.* **1981**, *74*, 1864−1872.
(69) Pratt, L. R.; Haan, S. W. *J. Chem. Phys.* **1981**, *74*, 1873−1876.
(70) Hummer, G.; Pratt, L. R.; Garcia, A. E.; Berne, B. J.; Rick, S. W. *J. Phys. Chem. B* **1997**, *101*, 3017−3020.
(71) Rossky, P. J.; Lee, S. H. *Chem. Scr.* **1989**, *29A*, 93−95.
(72) Wallqvist, A. *Chem. Phys. Lett.* **1990**, *165*, 437−442.
(73) Zhu, S. B.; Robinson, G. W. *J. Chem. Phys.* **1991**, *94*, 1403−1410;
(74) Lee, S. H.; Rossky, P. J. *J. Chem. Phys.* **1994**, *100*, 3334−3345.
(75) Shelley, J. C.; Patey, G. *N. Mol. Phys.* **1996**, *88*, 385−398.
(76) Feller, S. E.; Pastor, R. W.; Rojnuckarin, A.; Bogusz, S.; Brooks, B. R. *J. Phys. Chem.* **1996**, *100*, 17011−17020.
(77) Spohr, E. *J. Chem. Phys.* **1997**, *106*, 388−391.
(78) Spohr, E. *J. Chem. Phys.* **1997**, *107*, 6342−6348.
(79) Sakurai, M.; Tamagawa, H.; Ariga, K.; Kunitake, T.; Inoue, Y. *Chem. Phys. Lett.* **1998**, *289*, 567−571.
(80) Brodskaya, E.; Zakharov, V.; Laaksonen, A. *Langmuir* **2001**, *17*, 4443−4450.
(81) Borstnik, B.; Janezic, D. *J. Mol. Liq.* **1991**, *48*, 293−301.
(82) Vossen, M.; Forstmann, *F. J. Chem. Phys.* **1994**, *101*, 2379−2390.
(83) Booth, M. J.; Duh, D. M.; Haymet, A. D. J. *J. Chem. Phys.* **1994**, *101*, 7925−7933.
(84) Kinoshita, M.; Hirata, F. *J. Chem. Phys.* **1996**, *104*, 8807−8815.
(85) Bratko, D.; Curtis, R. A.; Blanch, H. W.; Prausnitz, J. M. *J. Chem. Phys.* **2001**, *115*, 3873−3877.
(86) Wallqvist, A.; Gallicchio, E.; Levy, R. M. *J. Phys. Chem. B* **2001**, *105*, 6745−6753.
(87) Galle, J.; Vörtler, H. L. *Surf. Sci.* **1999**, *421*, 33−43.
(88) Galle, J.; Vörtler, H. L. *Surf. Sci.* **2001**, *481*, 39−53.
(89) Berne, B. J.; Wallqvist, A. *Chem. Scr.* **1989**, *29A*, 85−91.
(90) Zhu, S. B. *Comp. Mater. Sci.* **1995**, *4*, 191−197.
(91) Hummer, G.; Garde, S.; Garcia, A. E.; Paulaitis, M. E.; Pratt, L. R. *Proc. Natl. Acad. Sci. U.S.A.* **1998**, *95*, 1552−1555.
(92) Kauzmann, W. *Nature* (*London*) **1987**, *325*, 763−764.
(93) Wilson, M. A.; Pohorille, A.; Pratt, L. R. *J. Phys. Chem.* **1987**, *91*, 4873−4878.
(94) Wilson, M. A.; Pohorille, A.; Pratt, L. R. *J. Chem. Phys.* **1988**, *88*, 3281−3285.
(95) Wilson, M. A.; Pohorille, A.; Pratt, L. R. *J. Chem. Phys.* **1989**, *90*, 5211−5213.
(96) Pratt, L. R. *J. Phys. Chem.* **1992**, *96*, 25−33.
(97) Yang, B.; Sullivan, D. E.; Tjipto-Margo, B.; Gray, C. G. *J. Phys.*: *Condens. Matter* **1991**, *3*, F109−F125.
(98) Yang, B.; Sullivan, D. E.; Gray, C. G. *J. Chem. Phys.* **1991**, *95*, 7777−7777.
(99) Matsumoto, M.; Kataoka, Y. *J. Chem. Phys.* **1989**, *90*, 2398−2407.
(100) Barraclough, C. G.; McTigue, P. T.; Ng, Y. L. *J. Electroanal. Chem.* **1992**, *329*, 9−24.
(101) Lie, G. C.; Grigoras, S.; Dang, L. X.; Yang, D. Y.; McLean, A. D. *J. Chem. Phys.* **1993**, *99*, 3933−3937.
(102) Ashbaugh, H. S. *Mol. Phys.* **1999**, *97*, 433−437.
(103) Hauttman, J.; Klein, M. L. *Mol. Phys.* **1992**, *75*, 379−395.
(104) Clark, A. T.; Madden, T. J.; Warren, P. B. *Mol. Phys.* **1996**, *87*, 1063−1069.
(105) Clark, A. T.; Madden, T. J.; Warren, P. B. *Mol. Phys.* **1997**, *92*, 947−947.
(106) Liem, S. Y.; Clarke, J. H. R. *Mol. Phys.* **1997**, *92*, 19−25.
(107) Grønbech-Jensen, N.; Hummer, G.; Beardmore, K. M. *Mol. Phys.* **1997**, *92*, 941−945.
(108) Widmann, A. H.; Adolf, D. B. *Comp. Phys. Commun.* **1997**, *107*, 167−186.
(109) Yeh, I. C.; Berkowitz, M. L. *J. Chem. Phys.* **1999**, *111*, 3155−3162.
(110) Grzybowski, A.; Gwozdz, E.; Brodka, A. *Phys. Rev. B* **2000**, *61*, 6706−6712.
(111) Wong, K. Y.; Pettitt, B. M. *Chem. Phys. Lett.* **2000**, *326*, 193−198.
(112) Kawata, M.; Mikami, M.; Nagashima, U. *J. Chem. Phys.* **2001**, *115*, 4457−4462.
(113) Kawata, M.; Nagashima, U. *Chem. Phys. Lett.* **2001**, *340*, 165−172.
(114) Kawata, M.; Mikami, M. *Chem. Phys. Lett.* **2001**, *340*, 157−164.
(115) Juffer, A. H.; Shepherd, C. M.; Vogel, H. J. *J. Chem. Phys.* **2001**, *114*, 1892−1905.
(116) Mountain, R. D. *J. Phys. Chem. B* **2001**, *105*, 6556−6561.
(117) Sokhan, V. P.; Tildesley, D. J. *Mol. Phys.* **1997**, *92*, 625−640.
(118) Motakabbir, K. A.; Berkowitz, M. L. *Chem. Phys. Lett.* **1991**, *176*, 61−66.
(119) Zhu, S. B.; Fillingim, T. G.; Robinson, G. W. *J. Phys. Chem.* **1991**, *95*, 1002−1006.
(120) da Rocha, S. R. P.; Johnston, K. P.; Westacott, R. E.; Rossky, P. J. *J. Phys. Chem. B* **2001**, *105*, 12092−12104.
(121) Vorholz, J.; Harismiadis, V. I.; Rumpf, B.; Panagiotopoulos, A. Z.; Maurer, G. *Fluid Phase Equilib.* **2000**, *170*, 203−234.
(122) Vassilev, P.; Hartnig, C.; Koper, M. T. M.; Frechard, F.; van Santen, R. A. *J. Chem. Phys.* **2001**, *115*, 9815−9820.
(123) Berendsen, H. J. C.; Grigera, J. R.; Straatsma, T. P. *J. Phys. Chem.* **1987**, *91*, 6269−6271.
(124) Guissani, Y.; Guillot, B. *J. Chem. Phys.* **1993**, *98*, 8221−8235.
(125) Alejandre, J.; Tildesley, D. J.; Chapela, G. A. *J. Chem. Phys.* **1995**, *102*, 4574−4583.
(126) dePablo, J. J.; Prausnitz, J. M. *Fluid Phase Equilib.* **1989**, *53*, 177−189.
(127) dePablo, J. J.; Prausnitz, J. M.; Strauch, H. J.; Cummings, P. T. *J. Chem. Phys.* **1990**, *93*, 7355−7359.
(128) Chen, B.; Xing, J. H.; Siepmann, J. I. *J. Phys. Chem. B* **2000**, *104*, 2391−2401.
(129) Svishchev, I. M.; Hayward, T. M. *J. Chem. Phys.* **1999**, *111*, 9034−9038.
(130) Yoshii, N.; Miyauchi, R.; Miura, S.; Okazaki, S. *Chem. Phys. Lett.* **2000**, *317*, 414−420.
(131) Mackie, A. D.; Hernandez-Cobos, J.; Vega, L. F. *J. Chem. Phys.* **1999**, *111*, 2103−2108.
(132) Guillot, B.; Guissani, Y. *J. Chem. Phys.* **1998**, *108*, 10162−10174.
(133) Bresme, F. *J. Chem. Phys.* **2001**, *115*, 7564−7574.
(134) Benjamin, I. *Chem. Rev.* **1996**, *96*, 1449−1475.
(135) Benjamin, I. *Annu. Rev. Phys. Chem.* **1997**, *48*, 407−451.
(136) Linse, P. *J. Chem. Phys.* **1987**, *86*, 4177−4187.
(137) Benjamin, I. *J. Chem. Phys* **1992**, *97*, 1432.
(138) Carpenter, I. L.; Hehre, W. J. *J. Phys. Chem.* **1990**, *94*, 531−536.
(139) Weeks, J. D. *J. Chem. Phys.* **1977**, *67*, 3106−3121.
(140) van Buuren, A. R.; Marrink, S. J.; Berendsen, H. J. C. *J. Phys. Chem.* **1993**, *97*, 9206−9212.
(141) Michael, D.; Benjamin, I. *J. Phys. Chem.* **1995**, *99*, 1530−1536.
(142) Zhang, Y. H.; Feller, S. E.; Brooks, B. R.; Pastor, R. W. *J. Chem. Phys.* **1995**, *103*, 10252−10266.
(143) Chang, T.; Dang, L. *J. Chem. Phys.* **1996**, *104*, 6772−6783.
(144) Senapati, S.; Berkowitz, M. L. *Phys. Rev. Lett.* **2001**, *87*, 6101-+.
(145) Eisenthal, K. *Annu. Rev. Phys. Chem.* **1992**, *43*, 627−661.
(146) Eisenthal, K. *Acc. Chem. Res.* **1993**, *26*, 636−643.
(147) Eisenthal, K. *Chem. Rev.* **1996**, *96*, 1343−1360.
(148) Miranda, P.; Shen, Y. *J. Phys. Chem. B* **1999**, *103*, 3292−3307.
(149) Gragson, D. E.; Richmond, G. L. *J. Phys. Chem. B* **1998**, *102*, 3847−3861.
(150) Shen, Y. R. Vibrational Spectroscopy for Water at Interfaces. In *Water in Biomaterials Surface Science*; Morra, M., Ed.; John Wiley & Sons. LTD.: New York, 2001.

(151) Richmond, G. *Annu. Rev. Phys. Chem.* **2001**, *52*, 357−389.
(152) Richmond, G. *Chem. Rev.* **2002**, *102*, 2693−2724.
(153) Benjamin, I. *Phys. Rev. Lett.* **1994**, *73*, 2083−2086.
(154) Sokhan, V. P.; Tildesley, D. J. *Faraday Discuss.* **1996**, *104*, 193−208.
(155) Morita, A.; Hynes, J. *Chem. Phys.* **2000**, *258*, 371−390.
(156) Conboy, J. C.; Daschbach, J. L.; Richmond, G. L. *Appl. Phys. A: Solids Surf.* **1994**, *59*, 623−629.
(157) Gragson; D. E.; Richmond, G. L. *Langmuir* **1997**, *13*, 4804−4806.
(158) Scatena, L. F.; Brown, M. G.; Richmond, G. L. *Science* **2001**, *292*, 908−912.
(159) Watry, M.; Brown, M.; Richmond, G. *Appl. Spectrosc.* **2001**, *55*, 321A−340A.
(160) Scatena, L. F.; Richmond, G. L. *J. Phys. Chem. B* **2001**, *105*, 11240−11250.
(161) Tikhonov, A.; Mitrinovic, D.; Li, M.; Huang, Z.; Schlossman, M. *J. Phys. Chem. B* **2000**, *104*, 6336−6339.
(162) Mitrinovic, D. M.; Tikhonov, A. M.; Li, M.; Huang, Z. Q.; Schlossman, M. L. *Phys. Rev. Lett.* **2000**, *85*, 582−585.
(163) Wilson, M. A.; Pohorille, A. *J. Am. Chem. Soc.* **1994**, *116*, 1490−1501.
(164) Venable, R.; Zhang, Y.; Hardy, B.; Pastor, R. *Science* **1993**, *262*, 223−226.
(165) Stouch, T. R. *Mol. Simul.* **1993**, *14*, 335.
(166) Damodaran, K. V.; Merz, Jr., K. M. *Biophys. J.* **1994**, *66*, 1076−1087.
(167) Essmann, U.; Perera, L.; Berkowitz, M. L. *Langmuir* **1995**, *11*, 4519−4531.
(168) Tu, K.; Tobias, D. J.; Blasie, J. K.; Klein, M. L. *Biophys. J.* **1996**, *70*, 595−608.
(169) Cascales, J. J. L.; delaTorre, J. G.; Marrink, S. J.; Berendsen, H. J. C. *J. Chem. Phys.* **1996**, *104*, 2713−2720.
(170) Feller, S. E.; Venable, R. M.; Pastor, R. W. *Langmuir* **1997**, *13*, 6555−6561.
(171) Feller, S.; Yin, D.; Pastor, R.; MacKerell, A. *Biophys. J.* **1997**, *73*, 2269−2279.
(172) Scott, H. L.; Jakobsson, E.; Subramanian, S. *Comput. Phys.* **1998**, *12*, 328−334.
(173) Armen, R. S.; Uitto, O. D.; Feller, S. E. *Biophys. J.* **1998**, *75*, 734−744.
(174) Chiu, S. W.; Clark, M. M.; Jakobsson, E.; Subramanian, S.; Scott, H. L. *J. Comput. Chem.* **1999**, *20*, 1153−1164.
(175) Essmann, U.; Berkowitz, M. L. *Biophys. J.* **1999**, *76*, 2081−2089.
(176) Feller, S. E.; Pastor, R. W. *J. Chem. Phys.* **1999**, *111*, 1281−1287.
(177) Feller, S. E.; Huster, D.; Gawrisch, K. *J. Am. Chem. Soc.* **1999**, *121*, 8963−8964.
(178) Venable, R. M.; Brooks, B. R.; Pastor, R. W. *J. Chem. Phys.* **2000**, *112*, 4822−4832.
(179) Lindahi, E.; Edholm, O. *Biophys. J.* **2000**, *79*, 426−433.
(180) Chiu, S. W.; Jakobsson, E.; Scott, H. L. *Biophys. J.* **2001**, *80*, 1104−1114.
(181) Tarek, M.; Tobias, D.; Chen, S.; Klein, M. *Phys. Rev. Lett.* **2001**, *8723*, 8101-+.
(182) Saiz, L.; Klein, M. *Biophys. J.* **2001**, *81*, 204−216.
(183) Murzyn, K.; Rog, T.; Jezierski, G.; Takaoka, Y.; Pasenkiewicz-Gierula, M. *Biophys. J.* **2001**, *81*, 170−183.
(184) Mashl, R.; Scott, H.; Subramaniam, S.; Jakobsson, E. *Biophys. J.* **2001**, *81*, 3005−3015.
(185) Feller, S.; Gawrisch, K.; MacKerell, A. *J. Am. Chem. Soc.* **2002**, *124*, 318−326.
(186) Smondyrev, A. M.; Berkowitz, M. L. *Biophys. J.* **1999**, 77, 2075−2089.
(187) Smondyrev, A: M.; Berkowitz, M. *L. Biophys. J.* **2000**, *78*, 1672−1680.
(188) Smondyrev, A. M.; Berkowitz, M. *L. Biophys. J.* **2001**, *80*, 1649−1658.
(189) Smondyrev, A.; Berkowitz, M. *Chem. Phys. Lipids* **2001**, *112*, 31−39.
(190) Schneider, M. J.; Feller, S. E. *J. Phys. Chem. B* **2001**, *105*, 1331−1337.
(191) Merz, K. M. *Curr. Opin. Struct. Biol.* **1997**, *7*, 511−517.
(192) Tieleman, D. P.; Marrink, S. J.; Berendsen, H. J. C. *Biochim. Biophys. Acta Rev. Biomembr.* **1997**, *1331*, 235−270.
(193) Forrest, L.; Sansom, M. *Curr. Opin. Struct. Biol.* **2000**, *10*, 174−181.
(194) Feller, S. E. *Curr. Opin. Colloid Interface Sci.* **2000**, *5*, 217−223.
(195) Nagle; J.; TristramNagle, S. *Biochim. Biophys. Acta Rev. Biomembr.* **2000**, *1469*, 159−195.
(196) Hristova, K.; White, S. *Biophys. J.* **1998**, *74*, 2419−2433.
(197) Feller, S.; Pastor, R. *Biophys. J.* **1996**, *71*, 1350−1355.
(198) Marrink, S. J.; Mark, A. E. *J. Phys. Chem. B* **2001**, *105*, 6122−6127.
(199) Pohorille, A.; Benjamin, I. *J. Phys. Chem.* **1993**, *97*, 2664−2670.
(200) Pohorille, A.; Wilson, M. A. *J. Chem. Phys.* **1996**, *104*, 3760−3773.
(201) Pohorille, A.; Cieplak, P.; Wilson, M. A. *Chem. Phys.* **1996**, *204*, 337−345.
(202) Chipot, C.; Wilson, M. A.; Pohorille, A. *J. Phys. Chem. B* **1997**, *101*, 782−791.
(203) Pohorille, A.; New, M. H.; Schweighofer, K.; Wilson, M. A. Computer simulations of small molecules in membranes. In *Membrane Permeability*: *100 years since Ernst Overton*; Deamer, D., Ed.; Current Topics in Membranes; Academic Press: San Diego, 1999.
(204) Pohorille, A.; Wilson, M. A.; Schweighofer, K. Electrostatic Properties of Aqueous Interfaces Probed by Small Solutes. In *Simulation and Theory of Electrostatic Interactions in Solution*; Pratt, L., Hummer, G., Eds.; AIP: New York, 1999.
(205) Marrink, S. J.; Berendsen, H. J. C. *J. Phys. Chem.* **1996**, *100*, 16729−16738.
(206) Xiang, T. X.; Anderson, B. D. *J. Chem. Phys.* **1999**, *110*, 1807−1818.
(207) Jedlovszky, P.; Mezei, M. *J. Am. Chem. Soc.* **2000**, *122*, 5125−5131.
(208) Bassolino-Klimas, D.; Alper, H. E.; Stouch, T. R. *Biochemistry* **1993**, *32*, 12624−12637.
(209) Bassolino-Klimas, D.; Alper, H. E.; Stouch, T. R. *J. Am. Chem. Soc.* **1995**, *117*, 4118−4129.
(210) Koubi, L.; Tarek, M.; Bandyopadhyay, S.; Klein, M. L.; Scharf, D. *Biophys. J.* **2001**, *81*, 3339−3345.
(211) Pierotti, R. A. *Chem. Rev.* **1976**, *76*, 717−726.
(212) Widom, B. *J. Chem. Phys.* **1963**, *39*, 2808−2812.
(213) Benjamin, I. *J. Chem. Phys.* **1992**, *96*, 577−585.
(214) Pohorille, A.; Wilson, M. A.; Chipot, C. *Prog. Colloid Polym. Sci.* **1997**, *103*, 29−40.
(215) Tu, K. C.; Tarek, M.; Klein, M. L.; Scharf, D. *Biophys. J.* **1998**, *75*, 2123-2134.
(216) Koubi, L.; Tarek, M.; Klein, M. L.; Scharf, D. *Biophys. J.* **2000**, *78*, 800−811.
(217) Diaz, M. D.; Fioroni, M.; Burger, K.; Berger, S. *Chem.-Eur. J.* **2002**, *8*, 1663−1669.
(218) Pohorille, A.; Wilson, M. A.; New, M. H.; Chipot, C. *Toxicol. Lett.* **1998**, *100-101*, 421−430.
(219) Cantor, R. S. *Biochemistry* **1997**, *36*, 2339−2344.
(220) Cantor, R. S. *J. Phys. Chem. B* **1997**, *101*, 1723−1725.
(221) Cantor, R. S. *Biophys. J.* **1999**, *76*, 2625−2639.
(222) Cantor, R. S. *Biophys. J.* **1999**, *77*, 2643−2647.
(223) Cantor, R. S. *Chem. Phys. Lipids* **1999**, *101*, 45−56.
(224) Qin, Z. H.; Szabo, G.; Cafiso, D. S. *Biochemistry* **1995**, *34*, 5536−5543.
(225) Cafiso, D. S. *Toxicol. Lett.* **1998**, *101*, 431−439.
(226) North, C.; Cafiso, D. S. *Biophys. J.* **1997**, *72*, 1754−1761.
(227) Tang, P.; Yan, B.; Xu, Y. *Biophys. J.* **1997**, *72*, 1676−1682.
(228) Baber, J.; Ellena, J. F.; Cafiso, D. S. *Biochemistry* **1995**, *34*, 6533−6539.
(229) Xu, Y.; Tang, P. *Biochim. Biophys. Acta* **1997**, *1323*, 154−162.
(230) Barry, J. A.; Gawrisch, K. *Biochemistry* **1994**, *33*, 8082−8088.
(231) Chipot, C.; Pohorille, A. *J. Phys. Chem. B* **1997**, *102*, 281−290.
(232) Pohorille, A.; Wilson, M. A. Interaction of a Model Peptide with a Water-Bilayer System. In *Structure and Reactivity in Aqueous Solution*: *Characterization of Chemical and Biological Systems*; Cramer, C., Truhlar, D., Eds.; ACS Symposium Series 568; American Chemical Society: Washington, D.C., 1994.
(233) Chipot, C.; Pohorille, A. *J. MAol. Struct.* (*THEOCHEM*) **1997**, *398*, 529−535.
(234) Petty, H. R. *Molecular Biology of Membrane Structure and Function*; Plenum Press: New York, 1993.
(235) Popot, J. L.; Engelman, D. M. *Annu. Rev. Biochem.* **2000**, *69*, 881−922.
(236) Von Heijne, G. *Annu. Rev. Biophys. Biomol. Struct.* **1994**, *23*, 167.
(237) Tamm, L. *Biochim. Biophys. Acta* **1991**, *1071*, 123−148.
(238) Kaiser, E. T.; Kezdy, F. J. *Ann. Rev. Biophys. Biophys. Chem.* **1987**, *16*, 561−581.
(239) Watts, A. *Biochim. Biophys. Acta* **1998**, *1376*, 297−318.
(240) Johansson, J.; Szyperski, T.; Curstedt, T.; Wfithrich, K. *Biochemistry* **1994**, *33*, 6015.
(241) Terzi, E.; Hdlzemann, G.; Seelig, J. *J. Mol. Biol.* **1995**, *252*, 633.
(242) Gazit, E.; Miller, I. R.; Biggin, P. C.; Sansomr, M. S. P.; Shai, Y. *J. Mol. Biol.* **1996**, *258*, 860−870.
(243) Cafiso, D. S. *Ann. Rev. Biophys. Biomol. Struct.* **1994**, *23*, 141−165.
(244) Dempsey, C. E. *Biochim. Biophys. Acta* **1990**, *1031*, 143−161.
(245) Wu, Y.; He, K.; Ludtke, S. J.; Huang, H. W. *Biophys. J.* **1995**, *68*, 2361−2369.
(246) Biggin, P. C.; Sansom, M. S. P. *Biophys. Chem.* **1996**, *60*, 99−110.
(247) Lear, J. D.; Schneider, J. P.; Kienker, P. K.; DeGrado, W. F. *J. Am. Chem. Soc.* **1997**, *119*, 3212−3217.
(248) Damodaran, K. V.; Merz, Jr., K. M.; Gaber, B. P. *Biophys. J.* **1995**, *69*, 1299−1308.
(249) Damodaran, K. V.; Merz, Jr., K. M. *J. Am. Chem. Soc.* **1995**, *117*, 6561−6571.
(250) Huang, P.; Loew, G. H. *J. Biomol. Struct. Dyn.* **1995**, *12*, 937−956.

(251) Chipot, C.; Pohorille, A. *J. Am. Chem. Soc.* **1998**, *120*, 11912−11924.
(252) Tieleman, D. P.; Berendsen, H. J. C.; Sansom, M. S. P. *Biophys. J.* **2001**, *80*, 331−346.
(253) Chipot, C.; Maigret, B.; Pohorille, A. *Proteins: Struct., Funct., Genet.* **1999**, *36*, 383−399.
(254) Ishiguro, R.; Kimura, N.; Takahashi, S. *Biochemistry* **1993**, *32*, 9792−9797.
(255) Bechinger, B.; Zasloff, M.; Opella, S. J. *Protein Sci.* **1993**, *2*, 2077−2084.
(256) Flach, C. R.; Brauner, J. W.; Taylor, J. W.; Baldwin, R. C.; Mendelsohn, R. *Biophys. J.* **1994**, *67*, 402−410.
(257) Blondelle, S. E.; Ostreh, J. M.; Houghten, R. A.; Perez-Paya, E. *Biophys. J.* **1995**, *68*, 351−359.
(258) Cornut, I.; Desbat, B.; Turlet, J. M.; Dufourcq, J. *Biophys. J.* **1996**, *70*, 305−312.
(259) DeGrado, W. F.; Lear, J. D. *J. Am. Chem. Soc.* **1985**, *107*, 7684−7689.
(260) Chung, L. A.; D., L. J.; DeGrado, W. F. *Biochemistry* **1992**, *31*, 6608−6616.
(261) Zangi, R.; DeVocht, M. L.; Robillard, G. T.; Mark, A. E. *Biophys. J.* **2002**, in press.
(262) Wymore, T.; Wong, T. *C. Biophys. J.* **1999**, *76*, 1199−1212.
(263) Keire, D. A.; Fletcher, T. G. *Biophys J.* **1996**, *70*, 1716−1727.
(264) Bradshaw, J. P.; Davies, S. M. A.; Hauss, T. *Biophys J.* **1998**, *75*, 889−895.
(265) Prevost, M.; Ortmans, I. *J. Phys. Chem. B* **2001**, *105*, 7080−7086.
(266) Shen, L.; Bassolino-Klimas, D.; Stouch, T. R. *Biophys. J.* **1997**, *73*, 3−20.
(267) Bern&che, S.; Nina, M.; Roux, B. *Biophys. J.* **1998**, *75*, 1603−1618.
(268) Ben-Tal, N.; Ben-Shaul, A.; Nicholls, A.; Honig, B. *Biophys. J.* **1996**, *70*, 1803−1812.
(269) Gao, X. F.; Wong, T. C. *Biopolymers* **2001**, *58*, 643−659.
(270) Engelman, D.; Steitz, T. A. *Cell* **1981**, *23*, 411−422.
(271) Popot, J. L.; Gerchman, S. E.; Engelman, D. M. *J. Mol. Biol.* **1987**, *198*, 655−676.
(272) Popot, J. L.; Engelman, D. M. *Biochemistry* **1990**, *29*, 4031−4037.
(273) Jacobs, R. E.; White, S. H. *Biochemistry* **1989**, *28*, 3421−3437.
(274) Sankararamakrishnan, R.; Weinstein, H. *Biophys. J.* **2000**, *79*, 2331−2344.
(275) Dalbey, R. E.; Kuhn, A.; Von Heijne, G. *Trends Cell Biol.* **1995**, *5*, 380−383.
(276) Duong, T.; Mehler, E.; Weinstein, H. *J. Comput. Phys.* **1999**, *151*, 358−387.
(277) Segrest, J. P.; DeLoof, H.; Dohlman, J. G.; Brouillette, C.; Anantharamaiah, G. *Proteins: Struct,. Funct., Genet.* **1990**, *8*, 103−117.
(278) Beckstein, O.; Biggin, P. C.; Sansom, M. S. P. *J. Phys. Chem. B* **2001**, *105*, 12902−12905.
(279) Hummer, G.; Rasaiah, J. C.; Noworyta, J. P. *Nature* **2001**, *414*, 188−190.
(280) Walther, J. H.; Jaffe, R.; Halicioglu, T.; Koumoutsakos, P. *J. Phys. Chem. B* **2001**, *105*, 9980−9987.
(281) Werder, T.; Walther, J. H.; Jaffe, R. L.; Halicioglu, T.; Noca, F.; Koumoutsakos, P. *Nano Lett.* **2001**, *1*, 697−702.

CR000692+